

0  
0  
0  
0  
0  
0  
0  
0  
AD A102688

LEVEL

12

AFGL-TR-81-0128

NEW TECHNIQUES AND DEVICES FOR MEASURING  
STRATOSPHERIC WINDS AND TURBULENCE

George P. Murphy

TRI-CON ASSOCIATES, INC.  
765 Concord Avenue  
Cambridge, Massachusetts 02138

Date of Report: May 1, 1981

FINAL REPORT: Period Covered June 1978  
To December 1980

DTIC  
REF ID: A6711  
AUG 11 1981  
C

Approved for Public Release, Distribution Unlimited

ONE FILE COPY

Air Force Geophysics Laboratories  
Air Force Systems Command  
United States Air Force  
Hanscom AFB, Massachusetts 01731

THIS DOCUMENT IS BEST QUALITY PRACTICABLE.  
THE COPY FURNISHED TO DDC CONTAINED A  
SIGNIFICANT NUMBER OF PAGES WHICH DO NOT  
REPRODUCE LEGIBLY.

81 8 10 034

Qualified requestors may obtain additional copies from  
the Defense Documentation Center. All others should apply  
to the National Technical Information Service.

## **DISCLAIMER NOTICE**

**THIS DOCUMENT IS BEST QUALITY  
PRACTICABLE. THE COPY FURNISHED  
TO DTIC CONTAINED A SIGNIFICANT  
NUMBER OF PAGES WHICH DO NOT  
REPRODUCE LEGIBLY.**

UNCLASSIFIED

SECURITY CLASSIFICATION OF THIS PAGE (When Data Entered)

(19) REPORT DOCUMENTATION PAGE		READ INSTRUCTIONS BEFORE COMPLETING FORM
1. REPORT NUMBER <i>(18) AFGI-TR-81-0128</i>	2. GOVT ACCESSION NO. <i>AD-A102680</i>	3. RECEIPT'S CATALOG NUMBER <i>(9)</i>
4. TITLE (and subtitle) <i>(9) NEW TECHNIQUES AND DEVICES FOR MEASURING STRATOSPHERIC WINDS AND TURBULENCE.</i>	5. TYPE OF REPORT & PERIOD COVERED <i>Final Report, Jun 1978 - Dec 1980</i>	
7. AUTHOR(s) <i>(10) George P. Murphy</i>	6. PERFORMING ORG. REPORT NUMBER <i>(14) C-170</i>	
9. PERFORMING ORGANIZATION NAME AND ADDRESS <i>TRI-CON ASSOCIATES, INC. 765 Concord Avenue Cambridge, MA 02138</i>	10. PROGRAM ELEMENT, PROJECT, TASK & WORK UNIT NUMBERS <i>(16) 62101F 668705AP (17) 05</i>	
11. CONTROLLING OFFICE NAME AND ADDRESS <i>AIR FORCE GEOPHYSICS LABORATORIES HANSCOM AIR FORCE BASE, MA 01731 CONTRACT MONITOR: J. H. Brown/LKD</i>	12. REPORT DATE <i>(11) 1 May 1981 (12) 73</i>	
14. MONITORING AGENCY NAME & ADDRESS (if different from Controlling Office)	15. SECURITY CLASS. (of this report) <i>UNCLASSIFIED</i>	
	15a. DECLASSIFICATION/DOWNGRADING SCHEDULE	
16. DISTRIBUTION STATEMENT (of this Report)  <i>Approved For Public Release, Distribution Unlimited</i>		
17. DISTRIBUTION STATEMENT (of the abstract entered in Block 20, if different from Report)		
18. SUPPLEMENTARY NOTES		
19. KEY WORDS (Continue on reverse side if necessary and identify by block number) <i>Corona Anemometer Time of Flight Anemometer Thermosonde Stratospheric Turbulence Stratospheric Winds</i>		
20. ABSTRACT (Continue on reverse side if necessary and identify by block number)  <i>New techniques and devices for Measuring Stratospheric Winds and Turbulence.</i>		

## TABLE OF CONTENTS

Paragraph	Page
1. INTRODUCTION AND OVERVIEW	1
1.1 Contract Specifications	1
2. CORONA ANEMOMETER	1
2.1 Description of Electronics	3
2.2 Review and Recommendations	7
3. TIME OF FLIGHT ANEMOMETER	11
3.1 Description of Operation	11
4. TWO DIMENSIONAL ANEMOMETER	14
4.1 Principal of Operation	14
4.2 Initial Tests and Results	14
5. THERMOSONDE	16
5.1 Thermosonde Circuit Description	17
6. LAUNCH SUPPORT	18
6.1 First Launch	19
6.2 Second Launch	20
6.3 Florida Launch	21
7. LABORATORY SUPPORT	21
7.1 Corona Anemometer	21
7.2 TOF Electrodes	22
7.3 Convective Heat Transfer Coefficient	22

Accession For	NTIS GRA&I
NTIS GRA&I	<input checked="" type="checkbox"/>
DTIC TAB	<input type="checkbox"/>
Unannounced	<input type="checkbox"/>
Justification	<input type="checkbox"/>
By	
Distribution/	
Availability Codes	
Dist	Avail and/or Special

APB

## LIST OF FIGURES

	Page
<b>FIGURE 1</b> Corona Anemometer	25
<b>FIGURE 2</b> Beam Displacement	26.
<b>FIGURE 3</b> Block Diagram Corona Anemometer	27
<b>FIGURE 4</b> Ion Current	28
<b>FIGURE 5</b> Pre-Amplifier Corona Anemometer	29
<b>FIGURE 6</b> Post-Amplifier Corona Anemometer	30
<b>FIGURE 7</b> Corona Current	31
<b>FIGURE 8</b> Digital Design	32
<b>FIGURE 9A</b> Time of Flight Anemometer	33
<b>FIGURE 9B</b> Time of Flight Anemometer	34
<b>FIGURE 10A</b> Pulse vs Count Rate	35
<b>FIGURE 10B</b> TOF Pulse vs Pressure	36

## LIST OF FIGURES

	Page
FIGURE 11 Log Amplifier TOF Anemometer	37
FIGURE 12 Pulse Shape	38
FIGURE 13 Thermosonde	39
FIGURE 14 Experimental Package	40
FIGURE 15 Gondola	41
FIGURE 16 Post Launch	42
FIGURE 17 Damaged Payload	43
FIGURE 18 Rebuilt Structure and Outriggers	44
FIGURE 19 Convective Heat Transfer Test Circuit	45
FIGURE 20 Two Dimensional TOF	46
FIGURE 5 (ADDENDUM A) Pre-Amp Transfer Functions	68

## INTRODUCTION OVERVIEW AND CONTRACT SPECIFICATIONS

### 1. INTRODUCTION AND OVERVIEW

This report covers the work performed on Contract No. F19628-78-C-0194 for the Air Force Geophysics Laboratory, Hanscom Air Force Base, Bedford, MA. The time period covered is from June 1978 to December 1980.

The instruments that were developed will be used to study stratospheric turbulence, which in turn, will help the scientist to understand the transport properties of aerosols and other pollutants in the upper atmosphere.

### 1.1 CONTRACT SPECIFICATIONS

- (a) To redesign modify and refurbish an existing AFGL Corona Anemometer and to provide field support for balloon launches at various sites within the USA.
- (b) To design and develop new techniques and devices for measuring stratospheric winds and turbulence.
- (c) To test and calibrate a time of flight anemometer using AFGL laboratory facilities.

### 2. CORONA ANEMOMETER

The primary instrument serviced under this contract is a Corona Anemometer, an instrument developed at AFGL to measure turbulence in the stratosphere.

An excellent description of the development and operation of the Corona Anemometer is available in a final report published by the Air Force Systems Command and referenced as AFGL-TR-78-0070.

To the reader who is not familiar with the Corona Anemometer, a brief description of the operation is as follows:

High voltage breakdown in a point to plane system is used to generate a corona current of a few micro-amps. Figure 1 page 25.

The plane in this instrument is a circular disc with a hole in the center to allow for ion extraction. The ions are then attracted to a target plate which is used to sense the beam displacement as a function of wind velocity.

The target plate is divided into four quadrants which are isolated from each other and have separate amplifiers to measure their portion of the ion beam.

Wind blowing perpendicular to the ion beam will cause a displacement similar to that shown in the illustration of Figure 2 on page 26.

By comparing in-flight results with a laboratory calibration, one can obtain pertinent data on wind profiles as a function of altitude and time.

## 2.1 DESCRIPTION OF ELECTRONICS

In Figure 3 on page 27, one can see a block diagram of the Corona Anemometer Experiment. An explanation of each of the subsystems will follow.

### 2.1.1 PRE-AMPLIFIERS

The pre-amplifiers are mounted in separate aluminum boxes to minimize noise and crosstalk effects on the low amplitude signals.

A Teledyne Philbrick 1425-02 FET integrated amplifier was chosen as the first stage of the preamplifier. The following specifications are pertinent:

$$V_{os} < 1 \text{ mv adjustable to zero}$$

$$I_{Bias} < 5 \text{ pa}$$

$$V_{os}/C_o < 10 \mu\text{v}/C_o$$

The low bias current is the primary reason for this selection. A table of ion current in each quadrant as a function of pressure appears in Figure 4 on page 28.

The operational amplifier is used in a voltage follower mode with an RC feedback network to set the upper frequency cutoff of approximately 1800 Hz.

If a redesign is done on the experiment, a different choice of operational amplifier could eliminate a number of components such as trim pots, resistors and capacitors.

It is also suggested to mount the pre-amps in the target housing to eliminate the need of long triax cables. These cables proved to be quite cumbersome. Using state of the art integrated circuits, a pre-amp could be mounted on a surface area no larger than  $10 \text{ cm}^2$ .

#### 2.1.2 POST AMPLIFIERS

The post-amplifiers are used to generate the X and Y components of the detected wind. The X component being  $\{(A+B)-(C+D)\}$  and the Y component  $\{(A+C)-(B+D)\}$ .

The ua 725 is used for low bias offset and low drift with temperature while the ua 741 is used for non critical general purpose amplification.

The output of the post-amplifier is sent to a divide block which conditions the signal by dividing  $K \{(A+B)-(C+D)\}$  by the product of pressure and total target current. The output of the divide block is sent back to the post-amplifier board and is used to generate the four telemetred signals: DC low, DC high, AC low and AC high. The DC high and AC high signals are a factor of ten higher than their respective low signals.

#### 2.1.3 ZERO CORRECTION

The zero correction circuit is used to compensate for drift or erroneous signals which may be due to changes in the ion beam characteristics resulting from needle point wear.

It will also detect and compensate for drift in the pre-amplifier and post-amplifier circuits.

On a command to "check zero", a motor driven cylinder moves to cover the opening between the sensor elements. This cover eliminates any air flow and results in a no wind condition. A signal is then sent to a one shot which resets the correction counter to zero and enables a square wave oscillator.

The oscillator and the counter produce a voltage staircase which is fed back to the post-amplifiers to correct for non zero conditions. When the zero level is reached, a comparator inhibits the oscillator, and the proper voltage level is stored in a counter. The starting point of the correction staircase is offset to eliminate the need for an up/down counter. The correction is made for both the X and Y directions. An indication of the correction voltage is also telemetred back to ground to serve as a diagnostic tool to determine the performance of the instrument.

#### 2.1.4 CORONA CURRENT CONTROL

The corona current control loop is made up of a high voltage power supply, an isolation amplifier and a voltage regulator. The current leaving the needle point causes a voltage to appear across a series resistor which serves as an input to the isolation amplifier. The isolation amplifier is a potted hybrid module. This module uses a high voltage isolated chopper transformer to transfer the sensed signal from the high voltage power supply output to the ground reference level. This signal is then used as a control of the high voltage by way of the input regulator. A rather long time constant (greater than 10 seconds) is inserted in the loop because of

the inherent instability of corona discharges. The corona current is adjusted in the laboratory by moving the needle point relative to the corona plate. The design goal 2 microamps of current with 1700 volts from point to plane is with a pressure of 120 mm Hg. The voltage necessary to maintain the 2  $\mu$ A will decrease as the experiment ascends into the stratosphere.

#### 2.1.5 MULTIPLY AND DIVIDE BLOCKS

To normalize the data as a function of altitude the output of a pressure transducer is multiplied by a signal indicating the total target current. The multiplier is of the analog type and performs the function:

$$E_o = \frac{E_{\text{pres}} E_{\text{tt}}}{10}$$

The output of the multiplier is then divided into the conditioned outputs of the post amplifiers to yield

$$X = \frac{K \{(A+B)-(C+D)\}}{K_2 (E_{\text{pres}} \times E_{\text{tt}})} \quad \text{and}$$

$$Y = \frac{K \{(A+C)-(B+D)\}}{K_2 (E_{\text{pres}} \times E_{\text{tt}})}$$

#### 2.1.6 HOUSEKEEPING

The remaining circuits are common to almost all experiments and include:

- (a) Voltage Regulators
- (b) Monitors
  - 1. Temperature
  - 2. Pressure
  - 3. Voltage
- (c) A commutator to time share the telemetry with slowly varying data.

## 2.2 REVIEW AND RECOMMENDATIONS

The AFGL Corona Anemometer as it exists today is rather large and heavy and consumes a considerable amount of power. This burden restricts its use to large scientific balloons. Its performance in the past has been satisfactory, but consideration should be given to a redesign in order to utilize the advances made in semiconductor technology. The redesign could follow an analog or digital format with the following recommendations.

### 2.2.1 ANALOG REDESIGN

#### 2.2.1.2 POWER SUPPLY AND REGULATORS

The regulator circuits are designed around the integrated circuit Module 723. This is one of the first integrated circuit voltage regulators produced and requires numerous external components. It also requires additional pass transistors if the load currents exceed fifty milliamps.

Fixed voltage regulators are now available, with a variety of voltages in a single package at different power ratings, and they usually require only two external capacitors.

The present design also uses several plus and minus voltages and a number of batteries to supply the power.

An alternate approach is to use a single battery and a DC to DC converter to generate the various voltages.

#### 2.2.1.2 ZERO CORRECTION

Due to the advances in digital to analog conversion techniques, the zero correction card may be greatly reduced. For example, converters are now available that have the counter, staircase generator, and buffer amplifier all in one dual-in-line package. The converters are available in 8, 10 and 12 bits with either binary or BCD codes.

#### 2.2.1.3 PRE-AMPLIFIERS

The location of the pre-amps relative to the four quadrant collectors requires an interface of costly and cumbersome triaxial cables and connectors. An alternate approach is to mount the pre-amps in the same housing as the collector plates. The new location would simplify the cable and should improve the signal to noise ratio.

#### 2.2.1.4 POST-AMPLIFIERS

The amplifier board utilizes 741 and 725 operational amplifiers to add, subtract, and amplify voltages from the pre-

amps. The 725 is not required in this application it could be replaced with an amplifier that is internally compensated thereby saving four components per amplifier.

Multiple amplifiers in the same package would also reduce the parts count without any loss in circuit performance. The trim potentiometers for the AC high, and AC low amplifiers are not necessary because of the inherent low offset voltage of these amplifiers. The overall reduction in parts would result in a board layout which is about one half the present size.

#### 2.2.1.5 MULTIPLY AND DIVIDE

The multiply and divide card uses modules that were manufactured with discreet components in a hybrid package. These modules were usually 1 1/2 to 2 inches square and approximately 1/2 inch high.

With the advance of integrated circuit technology, these same functions can be performed in a small T05 can and may be purchased for about one half the price.

#### 2.2.2 DIGITAL DESIGN

A digital design of a Corona Anemometer Experiment would incorporate the use of a microprocessor to perform the data handling and calculations that are presently being done with hybrid circuits.

The system would have the following subsystems: See Figure 8 page 32.

#### 2.2.2.1 PRE-AMPLIFIERS

The pre-amps increase the signal collected at each quadrant to a level compatible to the analog-to-digital converter.

#### 2.2.2.2 MULTIPLEXER

The multiplexer sequentially samples the data from each pre-amp and directs it to the analog-to-digital converter.

#### 2.2.2.3 ANALOG-TO-DIGITAL CONVERTER

Upon command from the microprocessor, the analog-to-digital converter converts the analog signal into 10 bits of digital data, and then stores the information until the processor has sampled each quadrant and the pressure transducer.

Rapid technological advancements in A/D converters are due to the developments of microprocessors and their need to communicate with analog signals.

Medium speed low power CMOS converters, which use the successive approximation principle, make 10 bit conversions in less than 10 microseconds.

#### 2.2.2.4 MICROPROCESSOR

The microprocessor is programmed to control the overall performance of the experiment and to calculate the various functions that are performed by analog circuits in the present design. These functions include addition, subtraction, multiplication and division.

When the shutter is closed, the microprocessor eliminates the zero correction circuit by sampling the output from each quadrant, and the results are stored in memory.

The processor then compares and calculates a correction factor. This factor is used until the next command for a zero check occurs..

The data out of the processor is in digital format and is telemetred back without the need of a PCM encoder. The word size is chosen so that the four most significant bits are an identification of the data to follow thus eliminating the need for synchronization.

### 3. TIME OF FLIGHT ANEMOMETER

#### 3.1 DESCRIPTION OF OPERATION

The TOF Anemometer was developed and used by various investigators in the pursuit of stratospheric wind measurements. The instrument is also referred to as a "Gas Flow" or "Ion Tracer" Anemometer. The operation (refer to Figure9) is as follows:

A high voltage spark causes ions to be created in the vicinity of the spark electrode. In the presence of a wind, the ions are moved down the tube to a collector which is biased to select the positive ions. If the distance is known and the time of transit can be established, the velocity can be calculated as follows:

$$V = \frac{S \times (\text{Clock})}{\text{Acc. Counts}}$$

Where:  $S$  = Distance between electrodes,  $\text{clock}$  = reference frequency,  $\text{Acc. Counts}$  = accumulated counts from start of pulse.

In the AFGL instrument, two TOF systems were mounted on the side of the balloon gondola. The vertical TOF contained two probes in the same tube to detect vertical or horizontal wind direction.

Sails were used to orientate the gondola in an attempt to point the horizontal TOF into the wind. The vertical TOF also gave an indication of the gondola's vertical motion during ballast or helium release.

### 3.1.1 CIRCUIT DESCRIPTION

### 3.1.2 PULSE GENERATION

The high voltage pulse was generated by way of a step up transformer with a turns ratio of 100: 1. The voltage amplitude is adjusted to about 2000 volts, and the pulse width is set at approximately 100 microseconds. The pulse rate is one pulse per second, and the timing is derived from the PCM encoder clock.

### 3.1.3 PULSE DETECTION

A transistor logarithmic amplifier is used to amplify the pulse upon its arrival at the collector. A logarithmic amplifier is used because of the wide variation in pulse amplitude resulting from diffusion. Pulses carried by low wind velocities appeared at the detector with lower amplitudes and broader widths because of the longer diffusing time. A series of photographs taken of actual pulses appears in Figure 10A and 10B on pages 35 and 36.

A calibration curve for the log amplifiers is shown in Figure 11 page 37 with the useful range of currents approximately  $5 \times 10^{-11}$  to  $10^{-7}$  amps.

### 3.1.4 PULSE TIMING

The pulse timing is accomplished by accumulating counts from a known clock source. The count begins when the high voltage pulse occurs, and it ends when the received pulse is detected.

To accurately measure the wind, the center of the pulse or the point at which the slope goes to zero is detected. The circuit designed to sense the zero slope included: a threshold detector to select all pulses over 0.25 volts; and a double differentiator followed by a zero crossing detector. The received pulse detector on the original experiments did not use the double differentiative method, therefore errors as large as 20 percent were common.

The accumulated counts were transferred into a 40 bit shift register and shifted out to telemetry at the proper time.

The 40 bits were utilized in the following manner:

- First 8 bits-Identification Code 10111000
- One bit-Detected Horizontal Pulse
- Fifteen bits-Horizontal Data
- One bit-Detected Vertical Pulse
- Fourteen bits-Vertical Data
- One bit-Up Or Down Vertical

## 4. TWO DIMENSIONAL TOF ANEMOMETER

### 4.1 PRINCIPLE OF OPERATION

The operation of the two dimensional TOF is similar to the previously mentioned instrument with the added capability of determining wind direction.

The ion cloud generation by means of a spark, and the timing and collection is basically the same as the one dimensional TOF. The collector, instead of being a piece of wire one-half inch long is a solid ring with a diameter of four inches covering 355 degrees.

Between the collecting ring and the ionizing electrode is another ring made up of segments. Each segment is electrically separated from the adjacent segment by a one meg-ohm resistor.

Each segment covers about five degrees of arc. The ends of the segmented ring serves as the input to a pair of integrating amplifiers, and the charge measured by each is used to determine wind direction.

### 4.2 INITIAL TESTS AND RESULTS

The first attempt at developing a circular or ring type of TOF Anemometer was done by using a glass tube. This tube was formed into a circle and coated with a resistive material. Another ring was fabricated by using a thin strip of printed circuit material. The copper was etched into segments and then formed into a ring. The segments were then connected to each other by one meg-ohm resistors.

The above mentioned sensors were tested in a bell jar at AFGL, and the results were compared to the one dimensional TOF.

The received pulse (Figure 12) of the circular TOF has a lower amplitude and broader peak. There was also an unwanted pulse, which is not velocity related, that occurs just after the high voltage discharge.

The unwanted pulse was at first attributed to poor grounding techniques, but additional testing seemed to prove otherwise.

Changing the bias on the collector through the range of -10 volts to +10 volts, caused both pulses to disappear (at  $\pm 2$  volts) and to reappear in the opposite polarity. These results are in agreement with previous experimenters, such as Lilienfeld et al, who claim the plasma cloud consists essentially of equal numbers of positive and negative ions.

Lilienfeld also had trouble with an unwanted spike, which occurred with the high voltage discharge, and he attributed this to very fast electrons.

The premature pulse in the circular TOF can be collected in either polarity. This indicates the presence of both positive and negative particles resulting from these very fast electrons.

These ions are generated by energetic electrons that produce a plasma in the vicinity of the collector, or by a secondary emission that strikes the collector.

The problem of an unwanted premature pulse could be solved by inhibiting the pulse detecting circuitry for about one millisecond after the high voltage discharge.

A new design with some different features is being fabricated and a sketch appears in Figure 20 page 46.

The new design will have a ground plane opposite the discharge electrode. This plate will reduce the effects of winds which are not in the plane of interest.

A dual ring will be used for ion collection. The first, a continuous ring which serves as the input to an amplifier, will be used to measure time. A second high impedance segmented ring will be used to measure charge distribution. The dual ring will be looking perpendicular to the air stream and will not be in the path of any energetic particles which originate at the spark electrode.

A bias on the collectors will be used to sample the plasma cloud as it moves over the collector.

## 5. THERMOSONDE

The thermosonde system was developed for the US Government by GTE Sylvania. This system measures temperature fluctuations in the atmosphere while being carried aloft on small weather balloons.

The temperature sensing elements are two fine wire probes separated by about one meter. The sensor material is Tungsten. The diameter is about 0.1 mil. and the length is approximately 0.5 cm.

The region of interest in temperature fluctuations is from  $.004^{\circ}\text{C}$  to about  $.4^{\circ}\text{C}$ .

The thermosonde will be integrated with a weather bureau type radiosonde, and the data returned to a ground station by way of the radiosonde transmitter.

The data from the thermosonde will be commutated with the data from three other sensors which measure pressure, temperature, and humidity.

### 5.1 THERMOSONDE CIRCUIT DESCRIPTION

A Block Diagram of the thermosonde circuit is shown in Figure 13. The probe resistance at  $25^{\circ}\text{C}$  is between 27 and 30 ohms. The change in probe resistance can be calculated by:

$$\Delta R = R_o \alpha \Delta T$$
$$= .00375 \text{ ohms.ohm}^{-1} \text{.DEG}^{-1}$$

(measured)

$$R_o = \text{Probe Resistance at } 0^{\circ}\text{C} = 25 \Omega$$

$$\Delta R = \text{For } .004^{\circ}\text{C}$$
$$= (.00375)(.004)(25\Omega)$$
$$= .00038\Omega$$

$$\Delta R = \text{For } .4^{\circ}\text{C}$$
$$= .038 \Omega$$

The signal levels over the region of interest at the bridge output are about 0.1 microvolts to 10 microvolts.

The bridge is driven by a three kilohertz sine wave and AC coupled to a high gain amplifier. The output of the amplifier is a sine wave whose amplitude is linearly related to the amount the bridge is unbalanced.

The signal output is then fed into a synchronous demodulator which recovers the signal without recognizing the DC offset drift of the amplifier.

The demodulator output is then filtered by a low pass 4 pole butterworth circuit which has a 3 dB cutoff frequency of about 1 kilohertz.

The filtered output is applied to an RMS operator whose output is telemetered back to ground. The future use of the thermosonde experiment will be in measuring the atmospheric refractive-index structure coefficient.

$$C_N^2 = \left( \frac{79 P(h)}{T^2(h)} \right) \times 10^{-6} \quad ^2 \times C_T^2(h)$$

P = Press in (mb)

T = Temperature (K)

and  $C_T$  is derived from thermosonde data. A photograph of the proposed experimental package is shown in Figure 14.

## 6. LAUNCH SUPPORT

The first launch support field trip for this contract involved traveling to Watertown, South Dakota, for measurement of wind turbulence over the plains.

A photograph of the gondola prior to launch appears in Figure 15. The scientific package consisted of two corona anemometers, two time of flight anemometers, a thermosonde experiment pressure transducer and a telemetry rack.

The balloon used for launch had a volume of approximately  $3 \times 10^6$  cubic feet and would take the payload up to about 90 thousand feet. Variations in altitude are adjusted by either releasing helium to descend or releasing a glass bead ballast to ascend.

After lift off, a reel down from the load bar allows the payload to float about 600 feet below the balloon and parachute, thereby, reducing the effects of the balloon on the turbulence sensor measurements. A sketch of the post launch configuration appears in Figure 16 page 42.

At the termination of flight (approximately 12 hours later) the balloon is separated from the rest of the payload, and a parachute controls the descending rate of the load bar and gondola.

Impact switches located in the base of the gondola are used to free the payload from the parachute upon touch-down.

#### 6.1 FIRST LAUNCH

The first launch from Watertown, South Dakota, was only a partial success because of power failure in the Corona Anemometer Experiment.

Examination of the housekeeping data indicated a high rate of discharge in one of the flight batteries with subsequent failure after about three hours of operation.

The payload was kept aloft for another four hours because all other experiments were functioning properly, mainly the TOF Anemometer.

When the balloon landed, the impact switches failed to activate. This failure caused the parachute to drag the gondola through a cornfield, and as a result of this failure, severe damage was inflicted upon the payload.

After assessing the damage, a decision was made to refurbish the gondola, to resume experimentation and to attempt another launch. Aluminum stock was then flown in from Minneapolis, and the upper structure and outriggers were completely rebuilt, see Figure 18 page 44.

## 6.2 SECOND LAUNCH

During the second balloon flight, the Corona Anemometers functioned properly, but the TOF experiments did not.

In the process of refurbishing the gondola, the TOF experiment was moved from a topside position to a lower portside position thus changing the amount of time the package received sunlight. The internal temperature of the TOF package during the first flight remained at about  $+50^{\circ}\text{F}$ , but during the second flight it dropped to  $-20^{\circ}\text{F}$ , resulting in a degradation of performance.

Data obtained from the two South Dakota flights added substantially to the knowledge of stratospheric winds.

### 6.3 FLORIDA LAUNCH

In August 1979, a high altitude balloon launch was made from Eglin Air Force Base in Florida. The balloon crossed the Gulf of Mexico and parachute landed in Texas. The purpose of the flight was to compare wind profiles and turbulences over the Gulf with data obtained over the plains and mountains.

The overall flight can be considered a success, but some minor problems did occur.

One of the two Corona Anemometers has a stability problem in the high voltage control loop which may have been caused by ice formation in the corona producing region.

The other Corona Anemometer functioned properly throughout the flight so that loss of data was minimal.

## 7. LABORATORY SUPPORT

In addition to launch support and experiment calibration, a variety of tasks were performed by TRI-CON personnel.

### 7.1 CORONA ANEMOMETER

A selection of aperture plates with various hole diameters and thicknesses were designed and manufactured to study the effects of electrode geometry on corona stability. A variety of needle points were also fabricated from different materials with machined tips at 30°, 45° and 60°.

A needle position control system was built using a stepping motor and gear box to simulate the change in corona characteristics as the needle tip wears down. The system can advance or retract the corona needle in .03 mil increments relative to a zero position.

## 7.2 TOF ELECTRODES

The TOF high voltage pulse did not always cause a breakdown at the spark electrode, when tests were being conducted in the laboratory. Occasionally, if the electrode was removed and polished with a final rinse in alcohol, the performance was improved.

There was never any indication of a misfire during either balloon flight, but reliability problems in the laboratory caused some concern.

Platinum iridium spheres, .02 inch in diameter were obtained from Engelhard Industries in New Jersey. An attempt to burn a hole in the spheres with a laser so that a lead could be attached turned out to be a failure. Investigations into the use of a noble metal such as platinum to make the TOF high voltage electrode has not been completed as of the termination of this contract.

## 7.3 CONVECTIVE HEAT TRANSFER COEFFICIENT

A circuit was designed to measure the thermal dynamic characteristic of the Tungsten wire which will be used in the thermosonde probes.

A Schematic of the circuit used is shown in Figure 19 and the operation is as follows:

Amplifier  $A_1$  is a voltage to current converter whose output current into the bridge circuit will be equal to the input voltage "Ein" divided by the selected resistor "Rs", within the limits of the power supply.

The bridge is made up of two precision wire wound resistors, a wire wound potentiometer and the probe under test.

The amount of unbalance in the bridge is amplified by  $A_2$  which has a gain of

$$g = 100/1.2 = 83.3$$

The wire wound resistors used in the bridge are purchased to a .01% tolerance and have a temperature coefficient of 2 ppm/ $^{\circ}\text{C}$ .

All other circuit parameters are relatively insensitive to temperature compared to the temperature coefficient of the Tungsten wire which is 3750 ppm/ $^{\circ}\text{C}$ .

The test is conducted by applying two known voltage levels to the input of  $A_1$  which produces two different current levels through the probe. For example, the two voltage levels of .5 volts and 5 volts would result in two currents of 1 ma and 10 ma.

The convective heat transfer coefficient can be calculated from the equation

$$h = \frac{I_2^2 R_2 - I_1^2 R_1}{JA_s \Delta T}$$

after  $\Delta T$  has been established from measured parameters and the standard  $\alpha$  of Tungsten.

$$\Delta R_1 = \frac{E_{o1}}{I_1}$$

$$\Delta R_2 = \frac{E_{o2}}{I_2}$$

$$\Delta R = \Delta R_2 - \Delta R_1$$

$$\Delta T = \frac{\Delta R}{(\alpha) R_p}$$

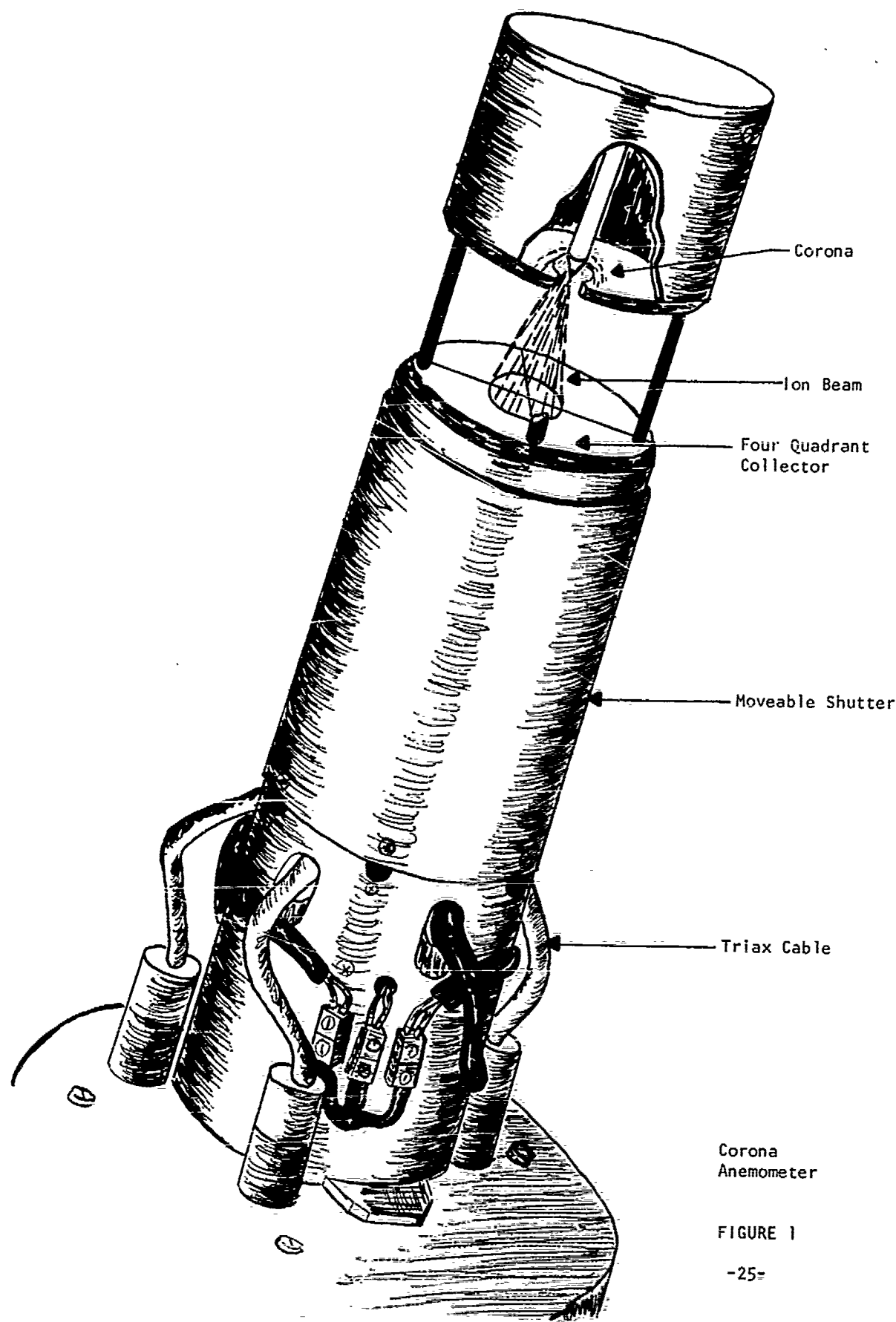


FIGURE 1

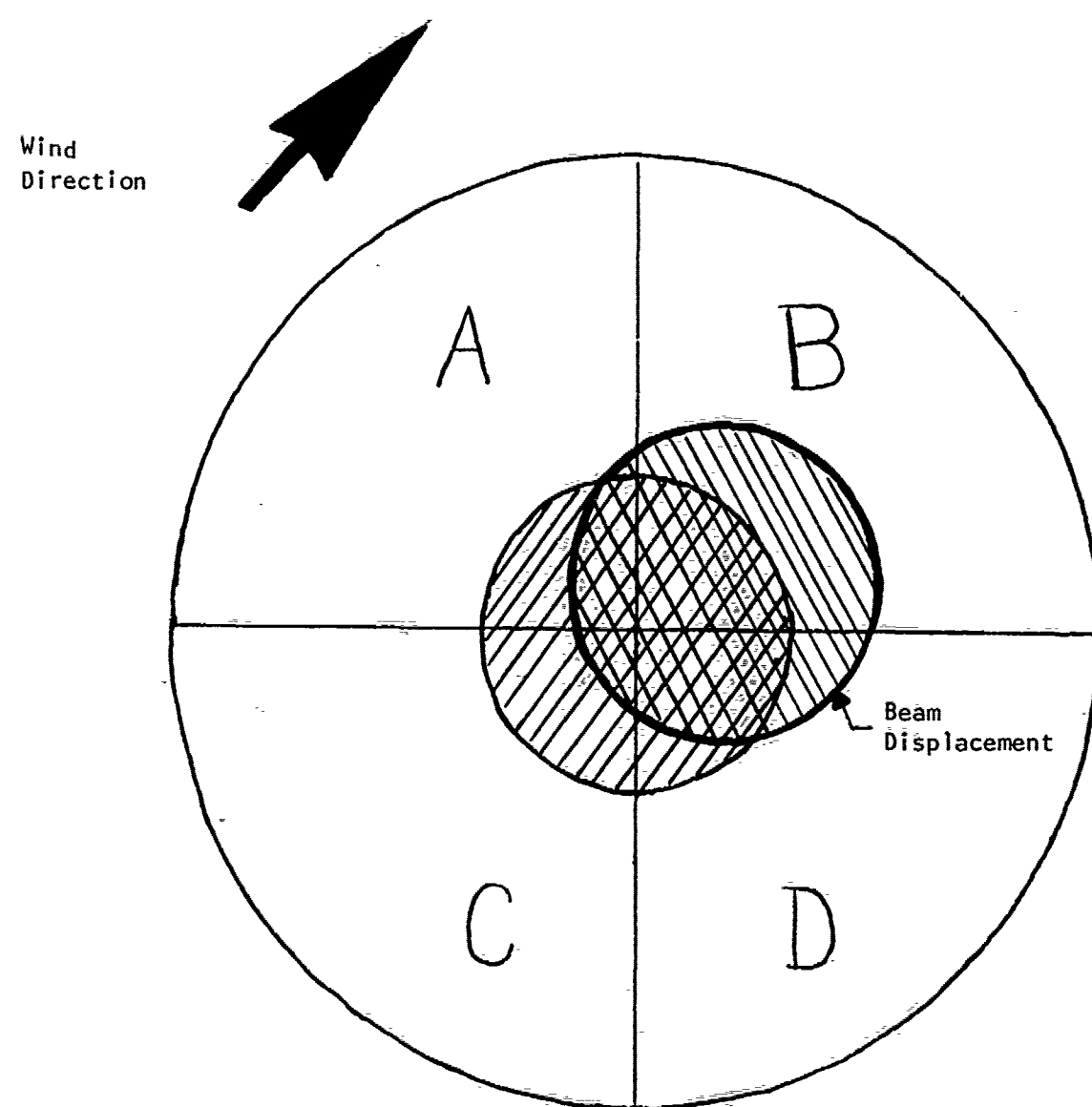
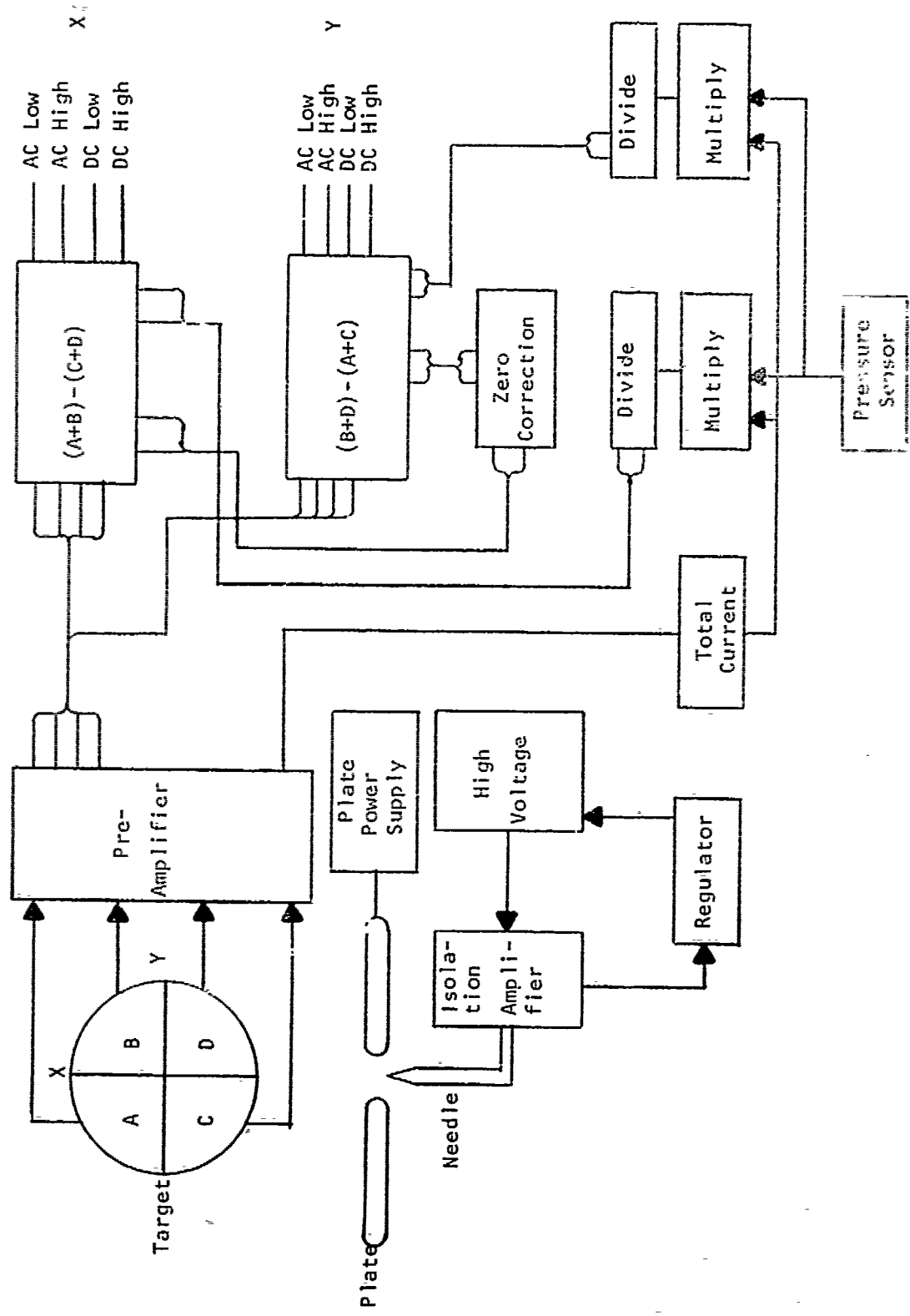


FIGURE 2



BLOCK DIAGRAM  
CORONA ANEMOMETER

FIGURE 3

Ion current as a function of pressure and bias voltage  
between corona plate and collector. Corona current =

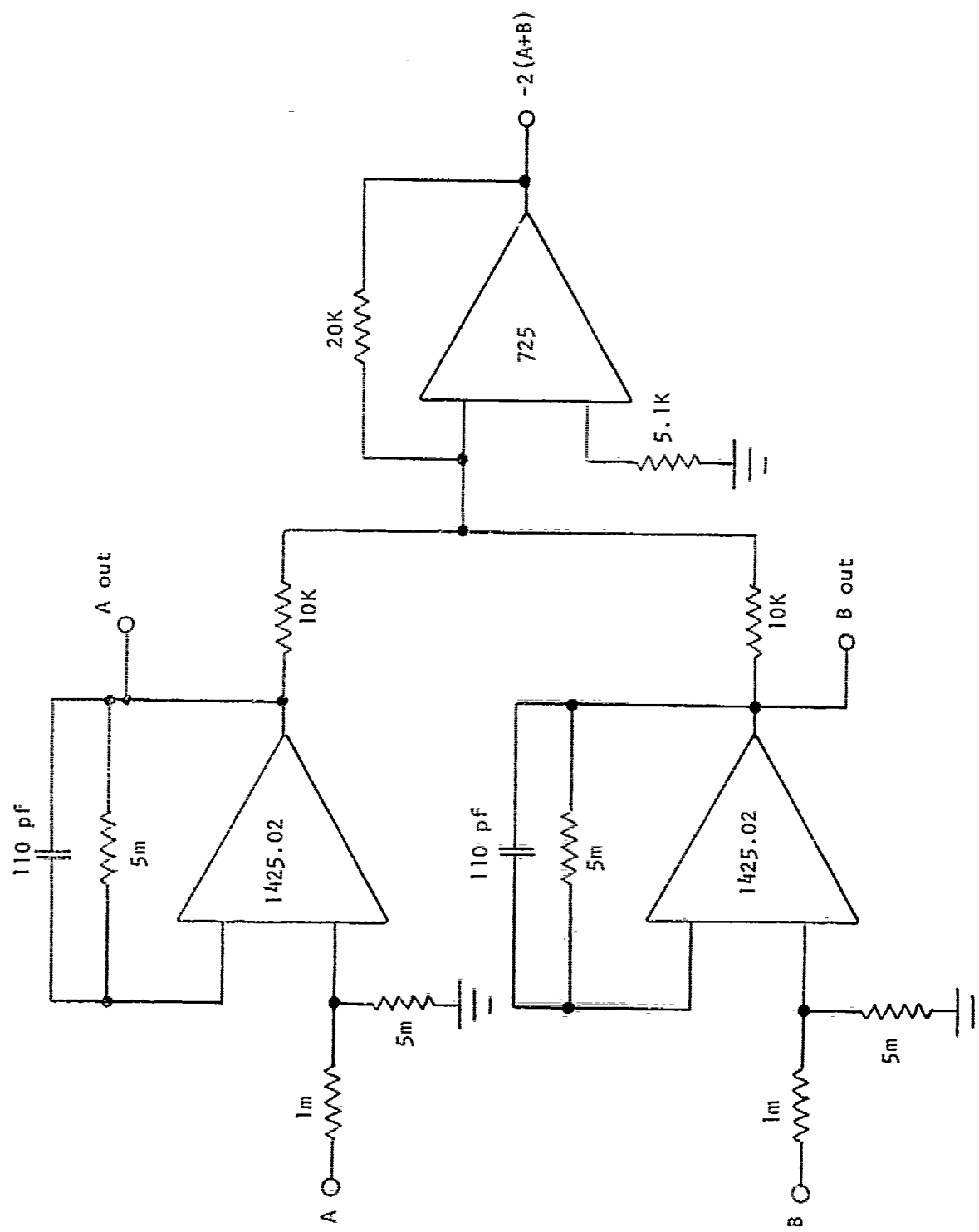
$P = 20 \text{ mm Hg}$

Plate Bias	100 volts	345 volts
Quad		
A	21.8 nano amps	131 nano amps
B	2.2 " "	130 " "
C	2.2 " "	132 " "
D	21.8 " "	130 " "

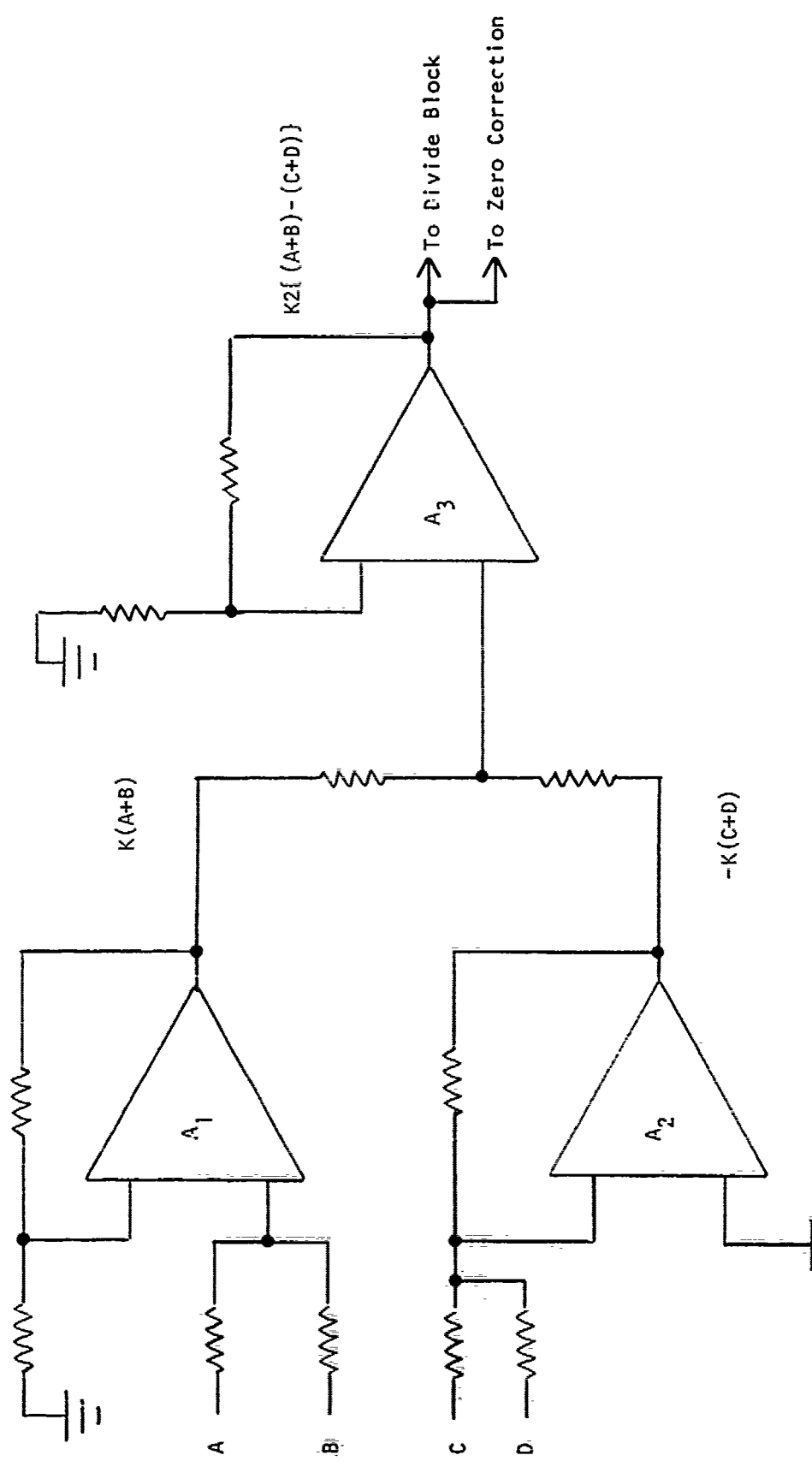
$P = 100 \text{ mm Hg}$

Plate Bias	100 volts	345 volts
Quad		
A	8 nano amps	38.8 nano amps
B	8 " "	39.2 " "
C	8 " "	38.6 " "
D	8 " "	38.8 " "

FIGURE 4

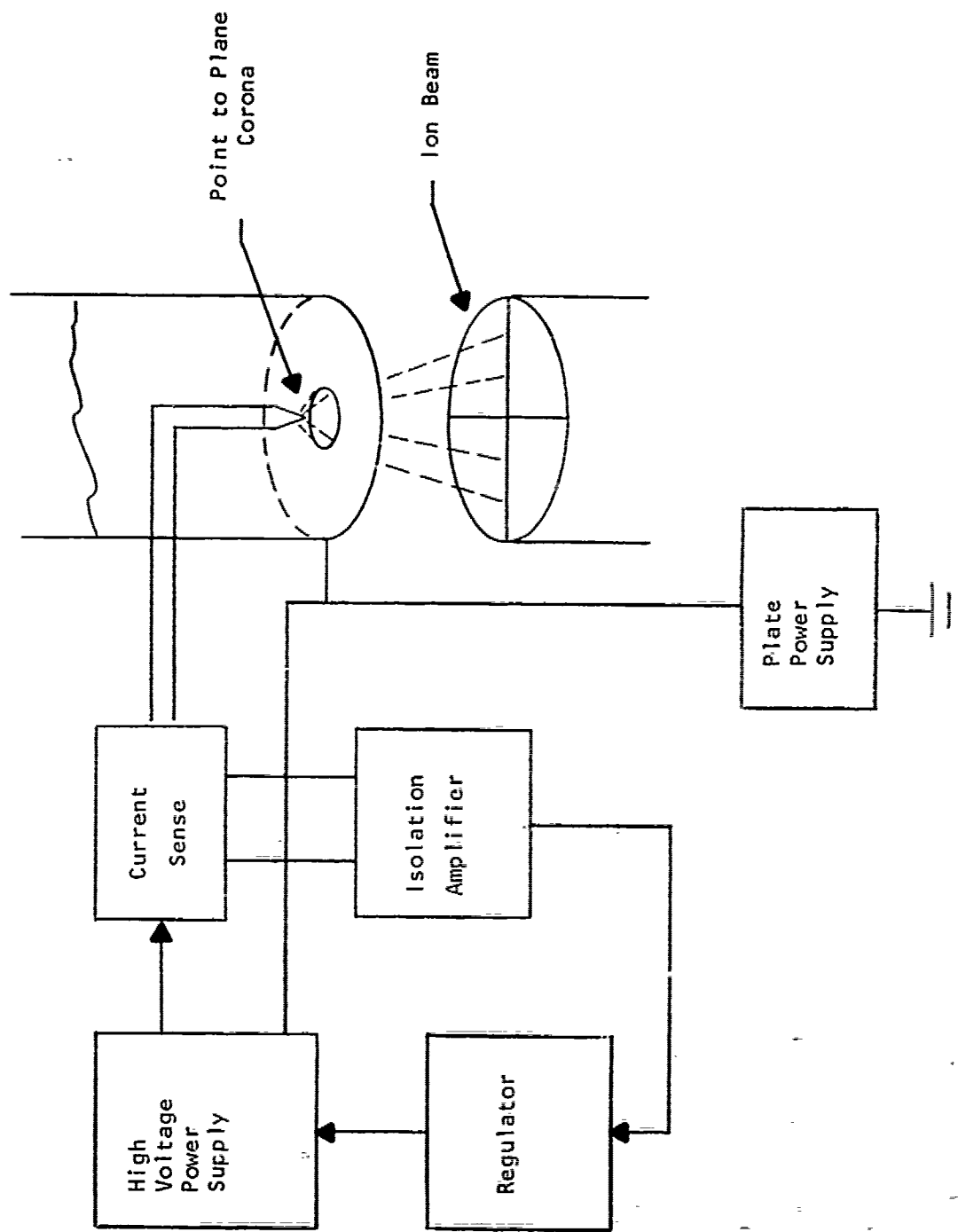


PRE-AMPLIFIER  
CORONA ANENOMETER  
FIGURE 5

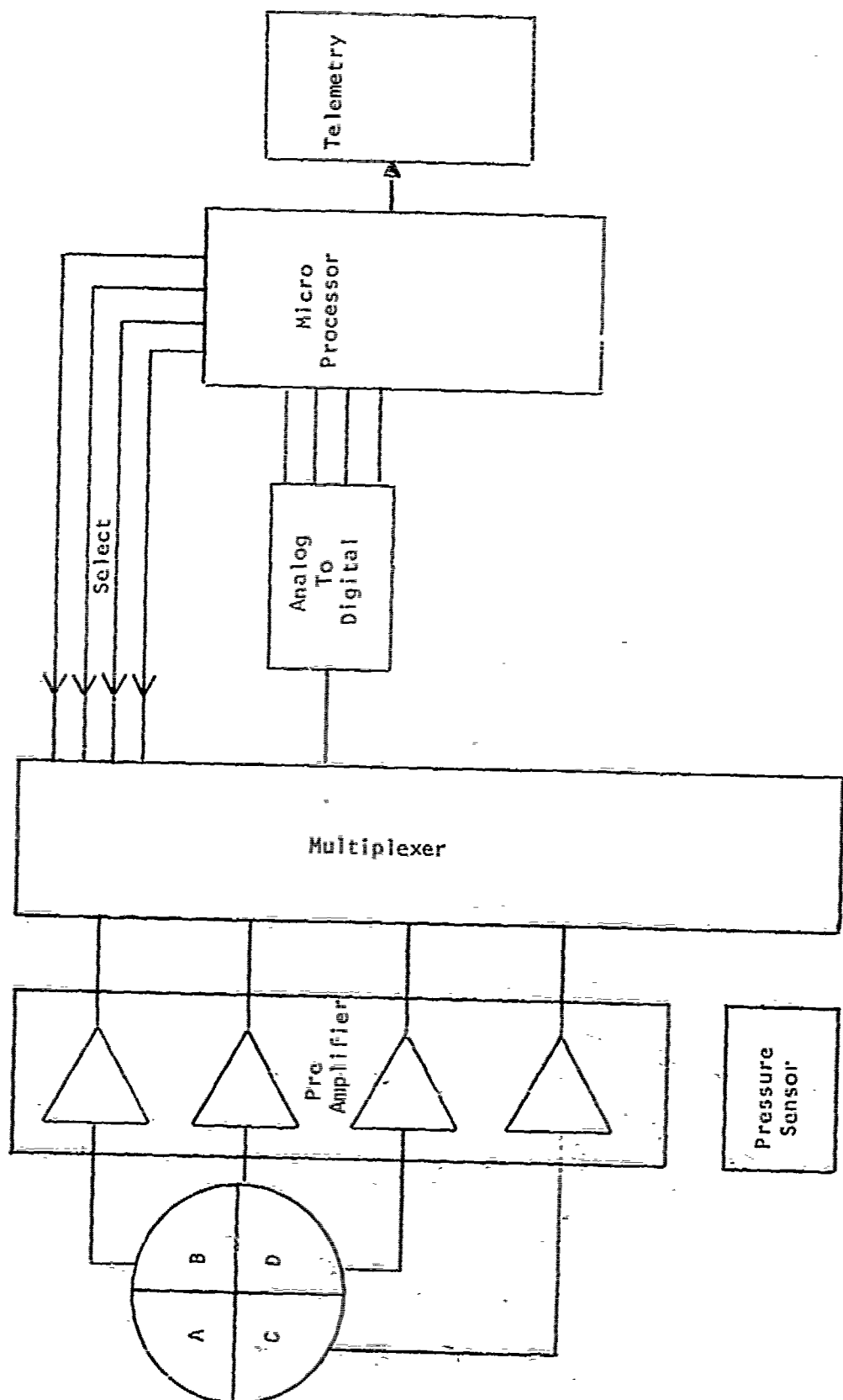


POST-AMPLIFIERS  
BLOCK DIAGRAM  
CORONA ANEMOMETER

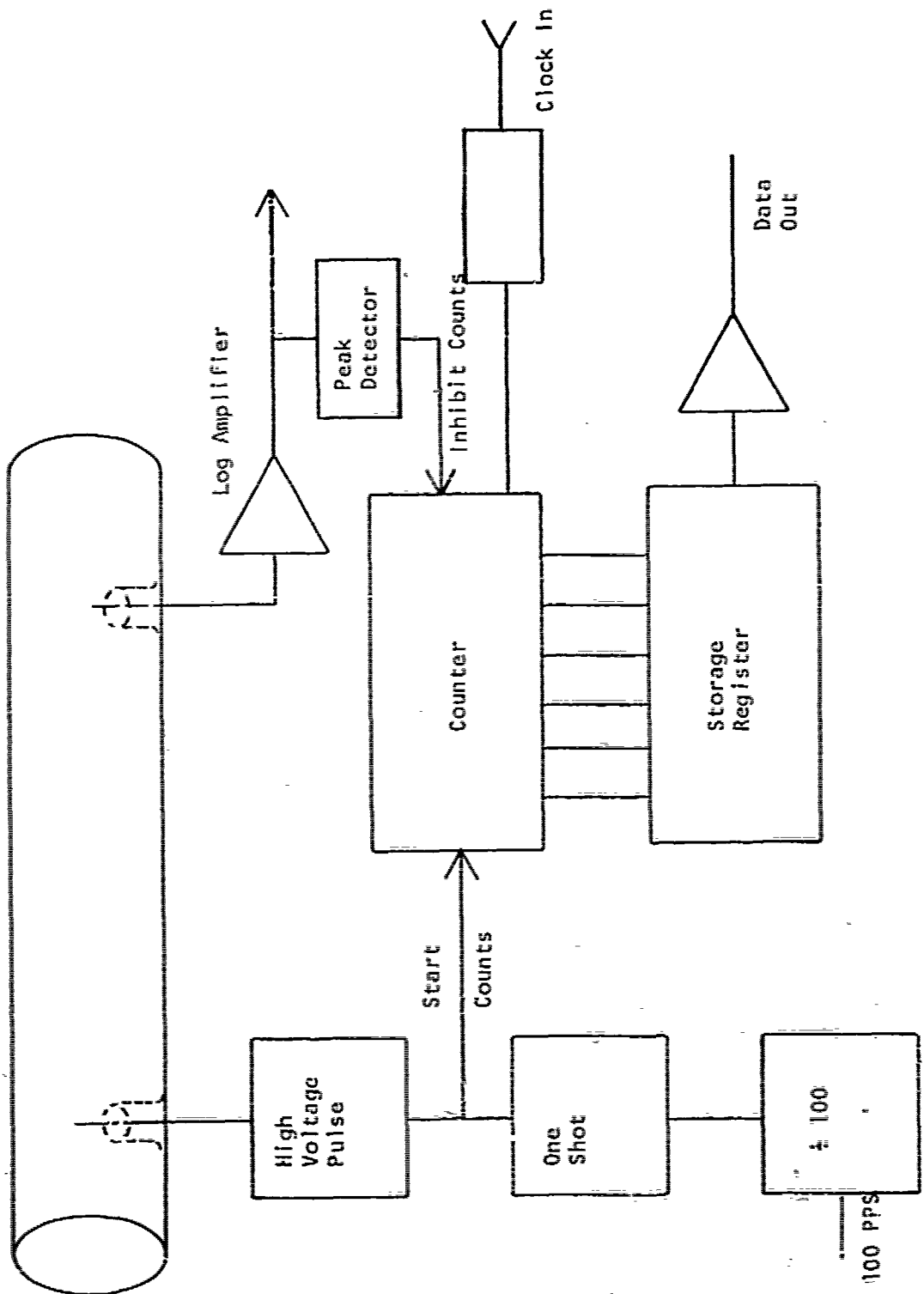
FIGURE 6



CORONA CURRENT  
FIGURE 7

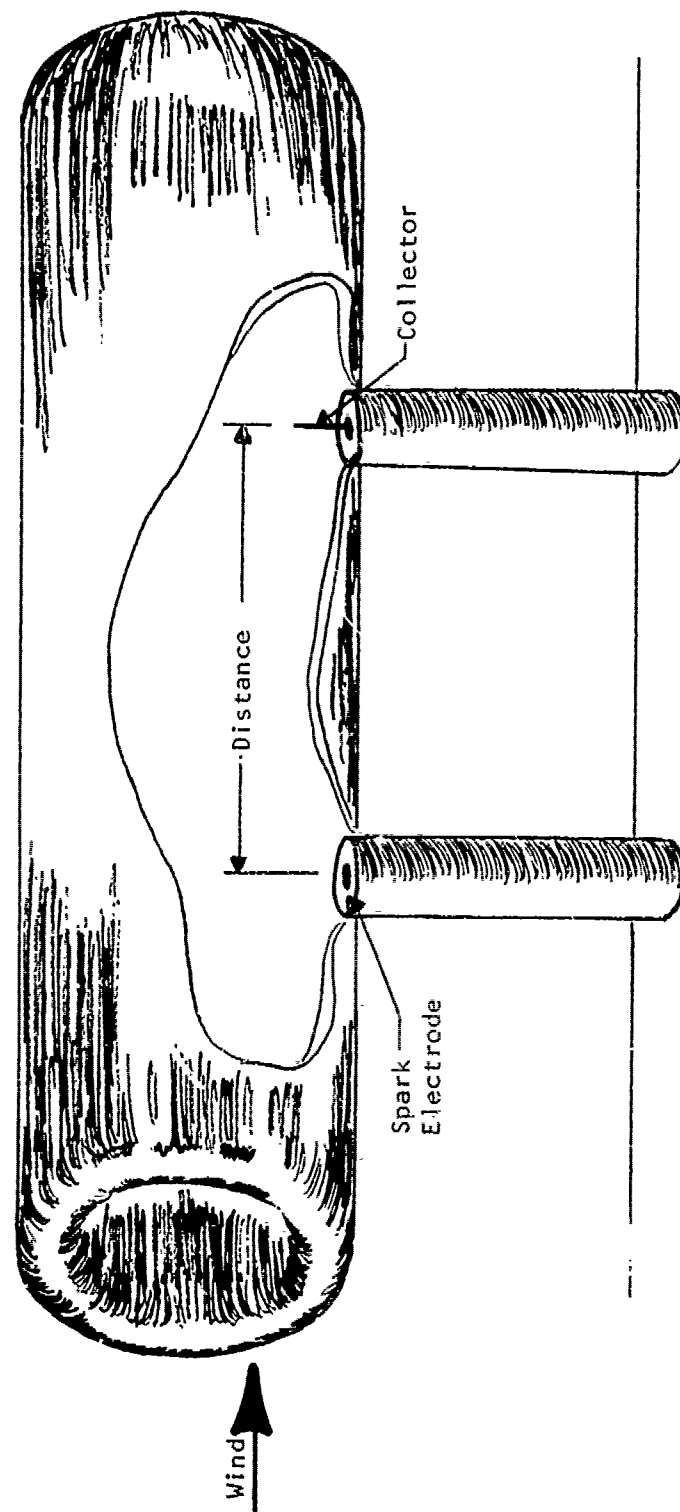


DIGITAL DESIGN  
BLOCK DIAGRAM  
FIGURE 8

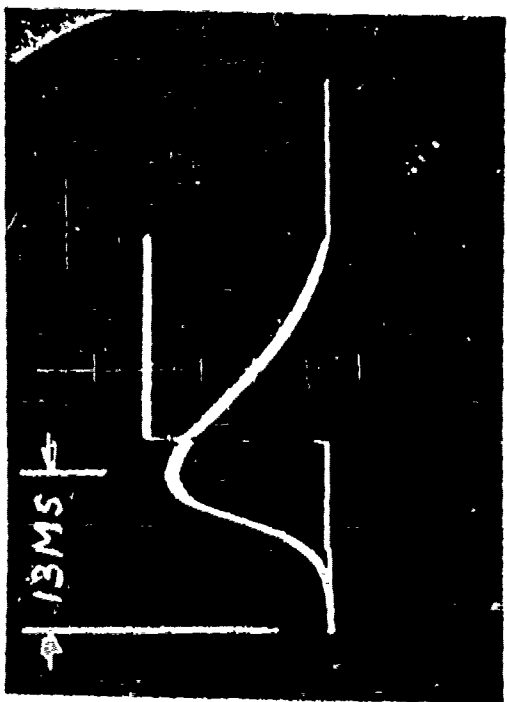


TIME OF FLIGHT  
ANEMOMETER  
BLOCK DIAGRAM

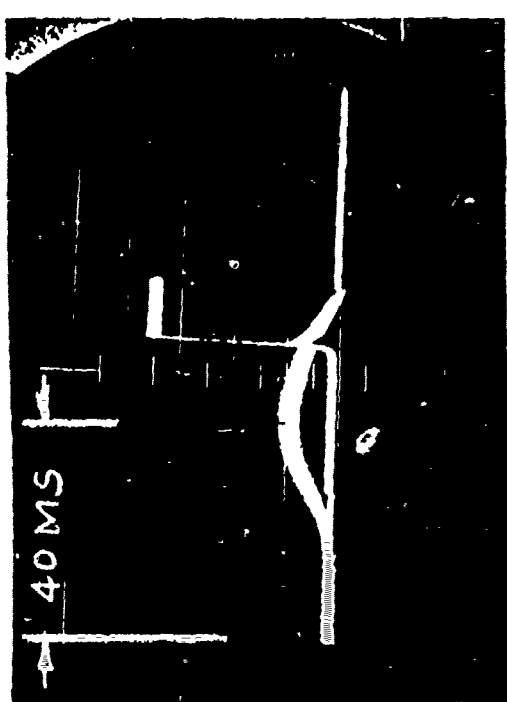
FIGURE 9A



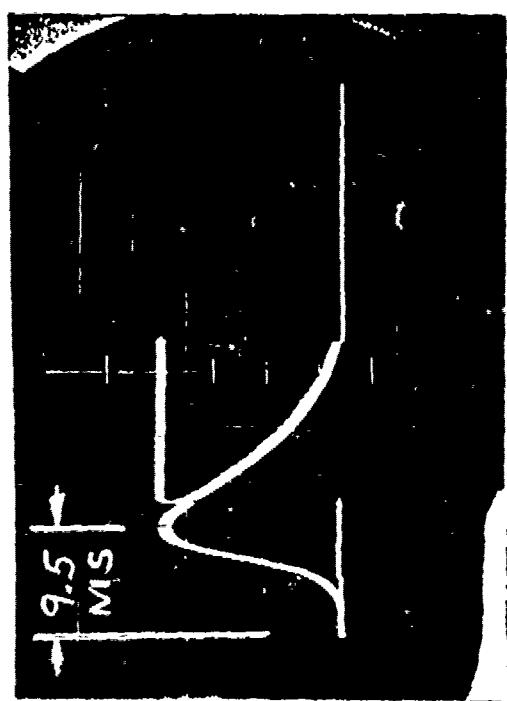
TIME OF FLIGHT ANEMOMETER  
FIGURE 9B



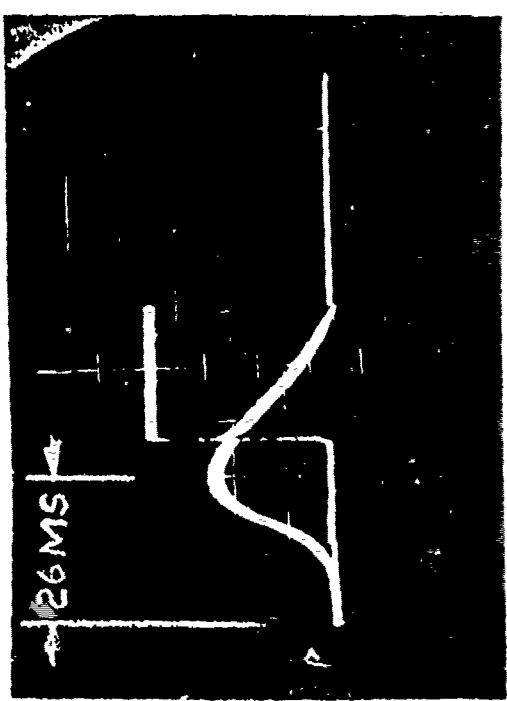
$I_{Peak} = 3 \times 10^{-9} A$  600 counts/sec.



$I_{Peak} = 10^{-10} A$  200 counts/sec.

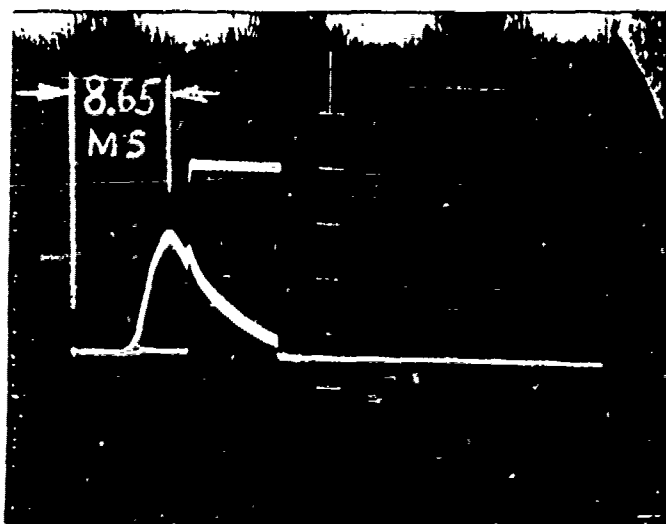


$I_{Peak} = 5 \times 10^{-9} A$  800 counts/sec.

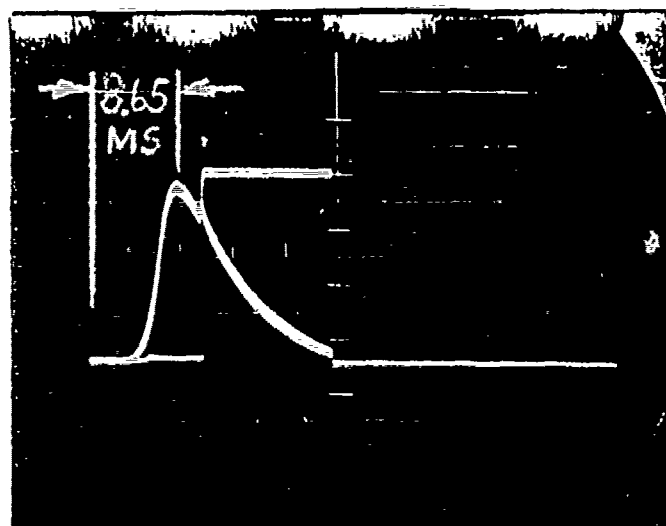


$I_{Peak} = 10^{-9} A$  400 counts/sec.

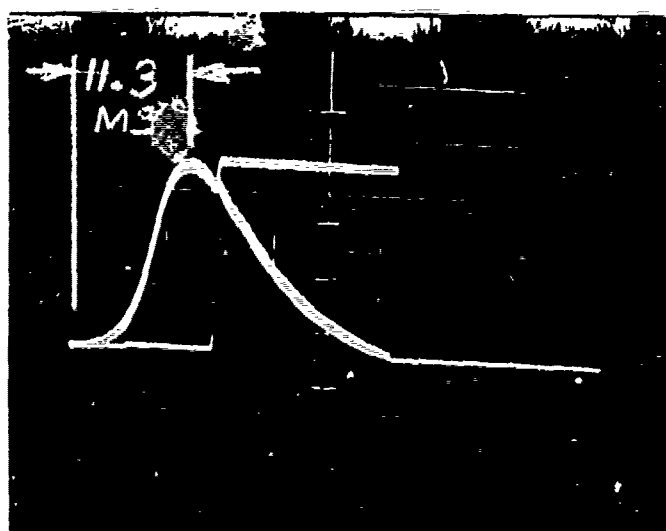
PULSE VS COUNT RATE  
PRESSURE = 20 mm Hg  
FIGURE = 10A



Pres = 60 mm Hg  
 $I_{Peak} = 7 \times 10^{-10} A$



Pres = 30 mm Hg  
 $I_{Peak} = 5 \times 10^{-9} A$



Pres = 15 mm Hg  
 $I_{Peak} = 7 \times 10^{-9} A$

BLOWER SPEED = 800 Counts/sec

TOF PULSE vs Pressure

FIGURE 10B

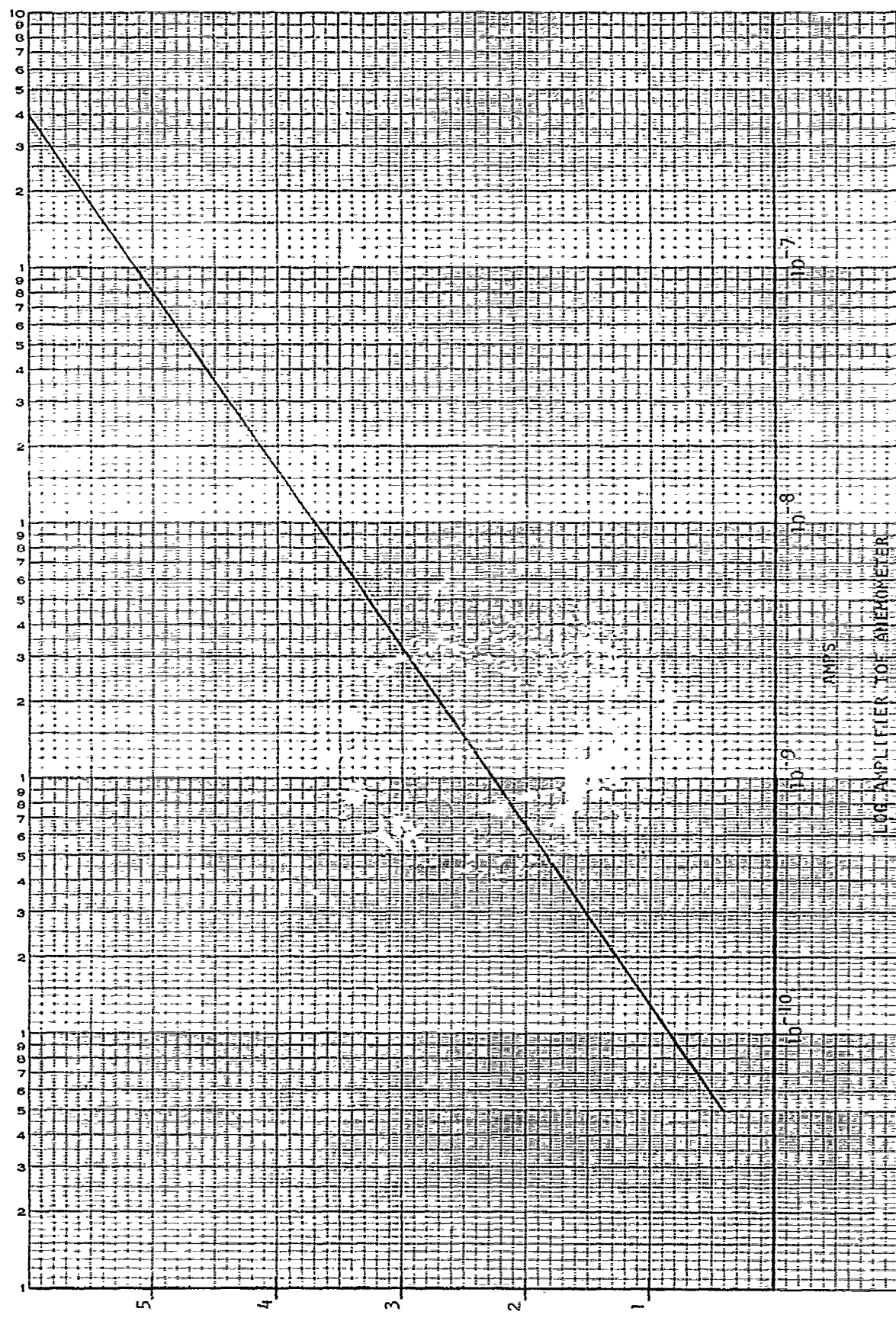
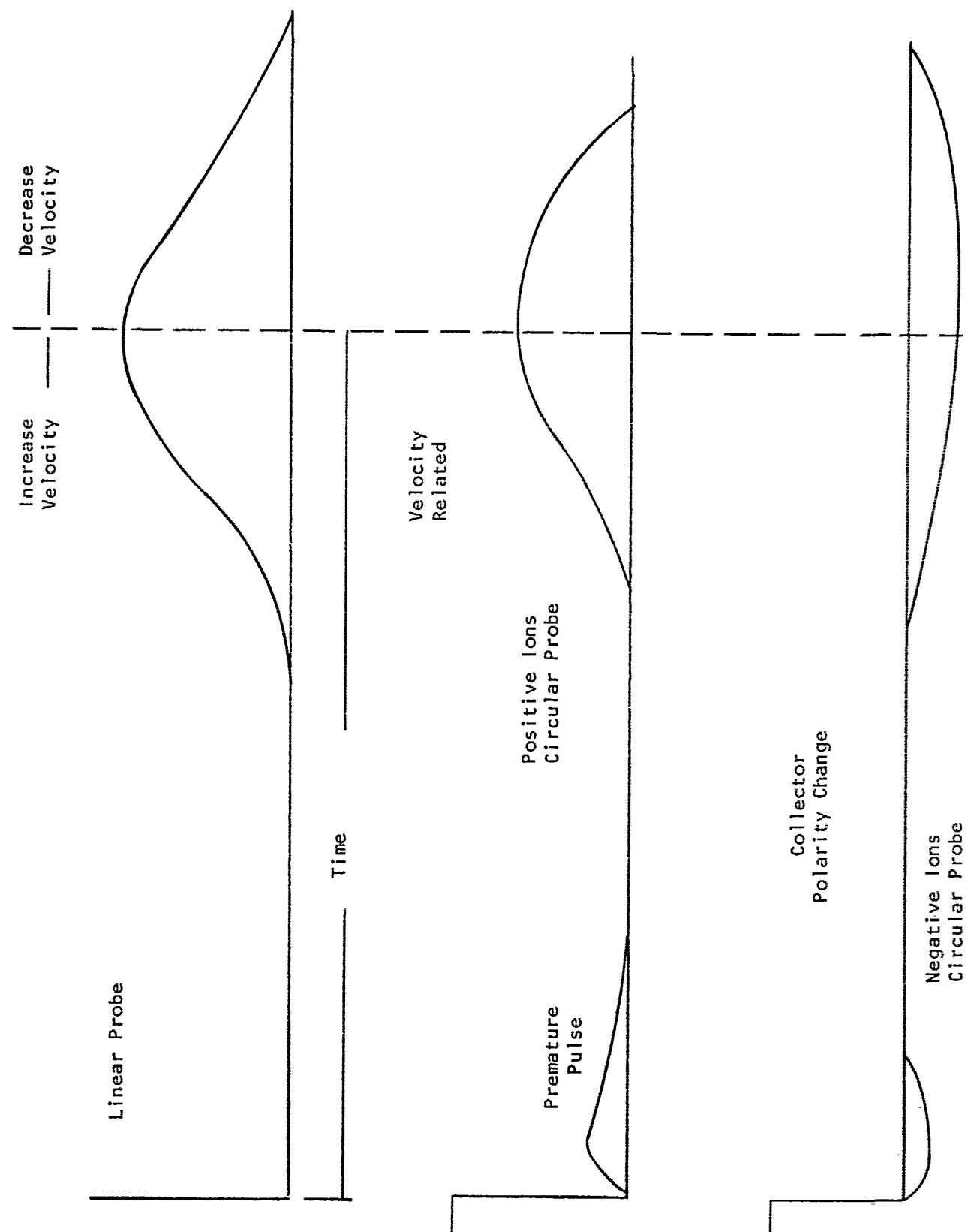
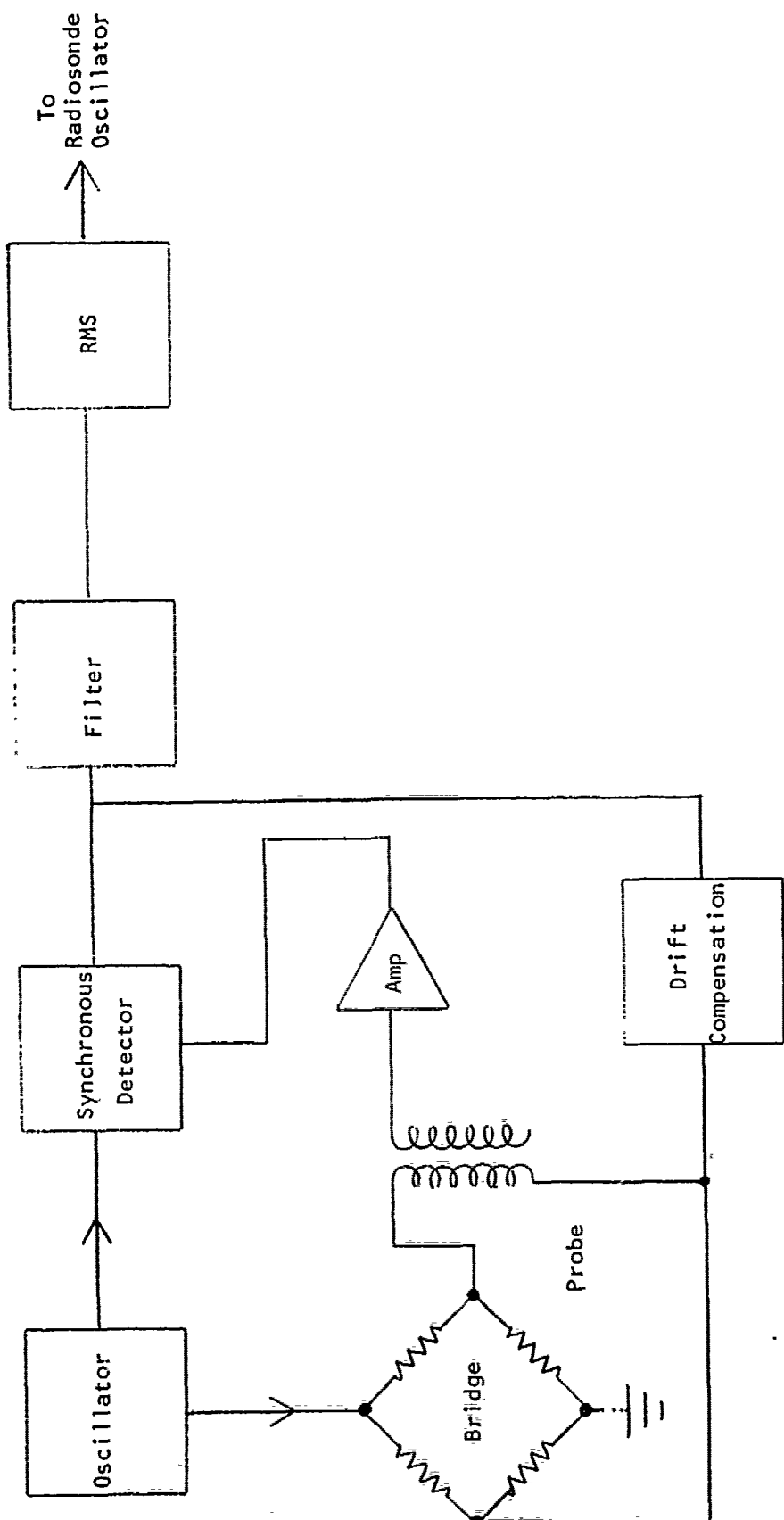


FIGURE 11



PULSE SHAPE  
TIME OF FLIGHT ANEMOMETER

FIGURE 12



THERMOSONDE BLOCK DIAGRAM  
FIGURE 13

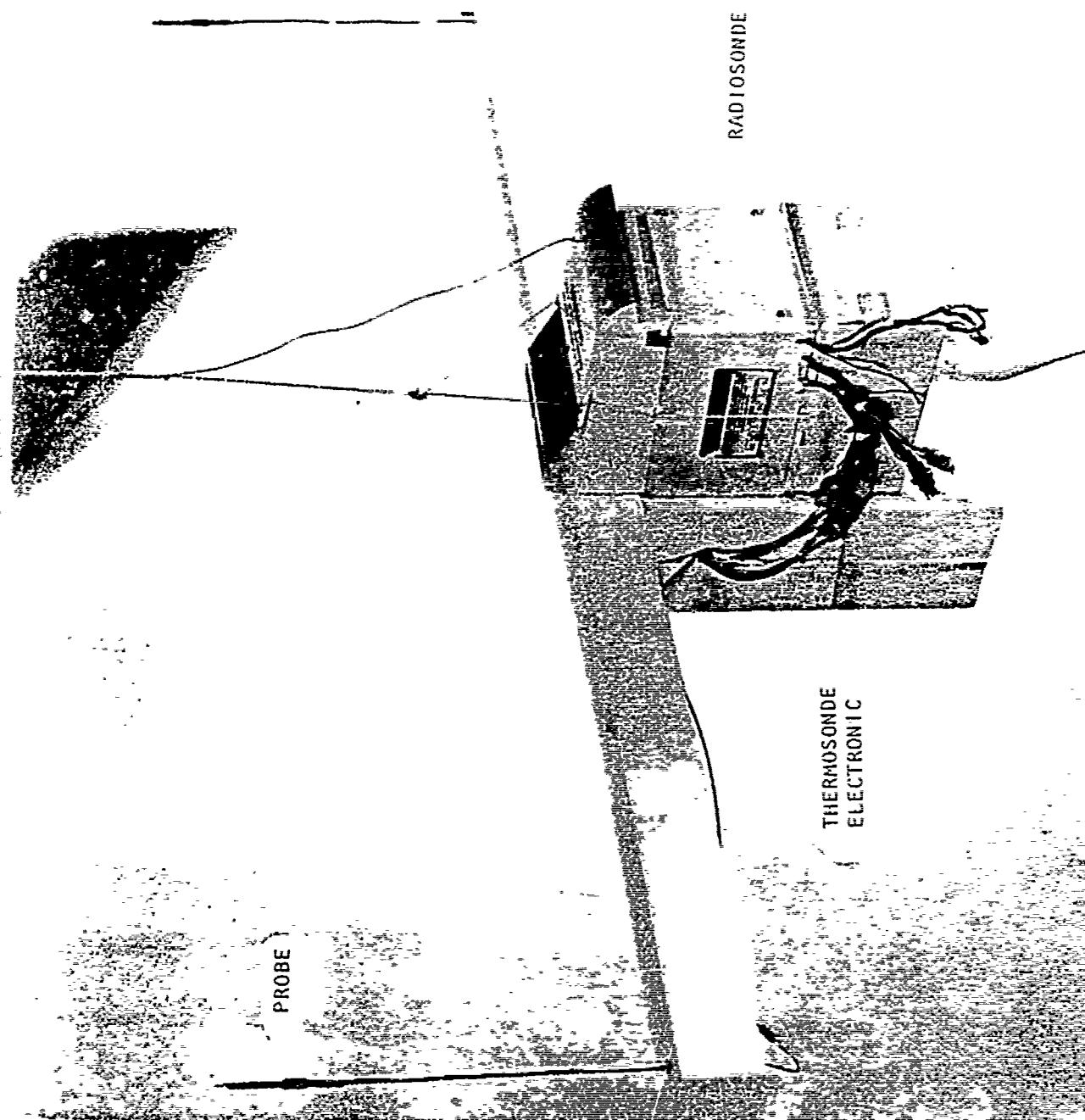


FIGURE 14

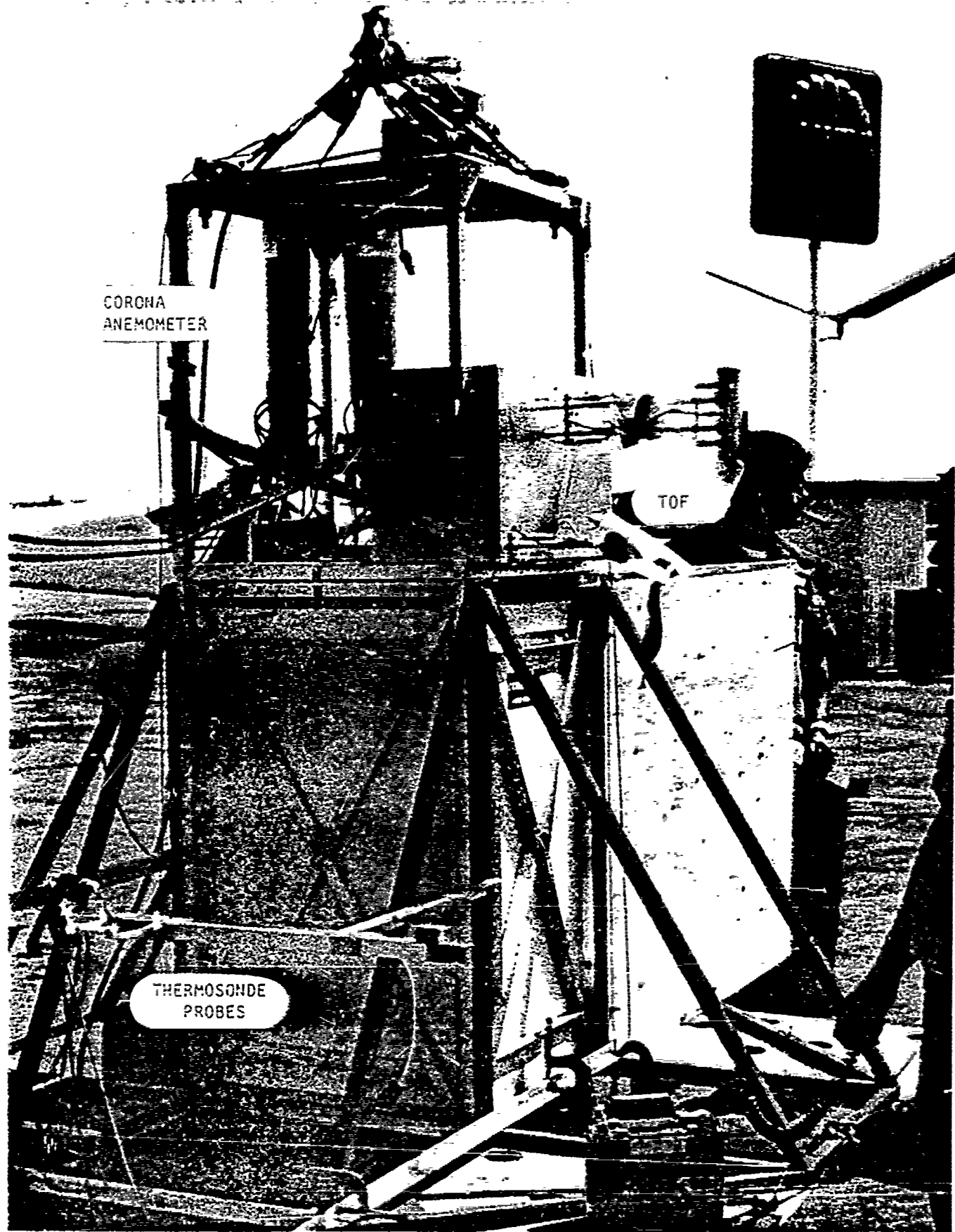


FIGURE 15

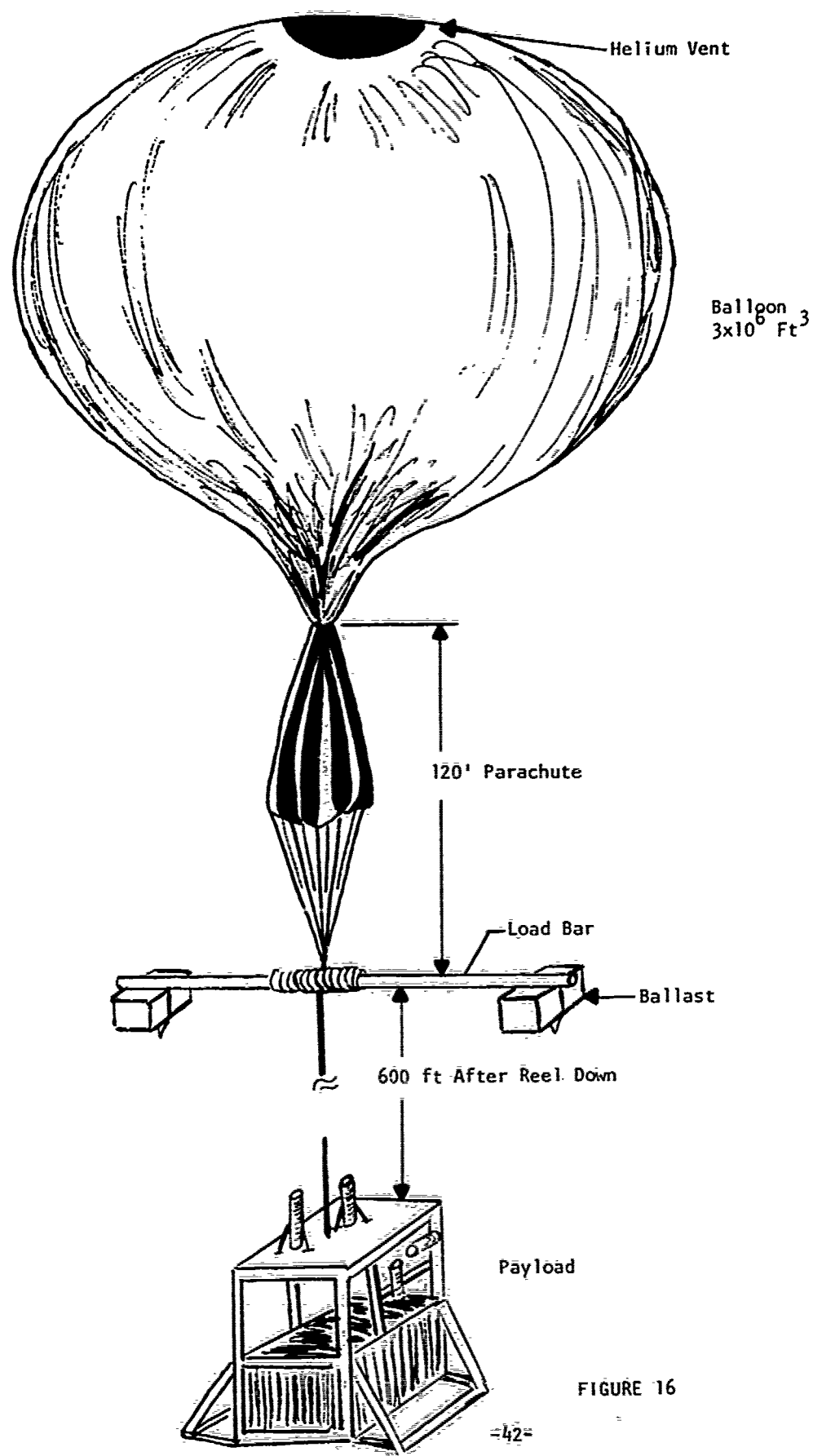


FIGURE 16

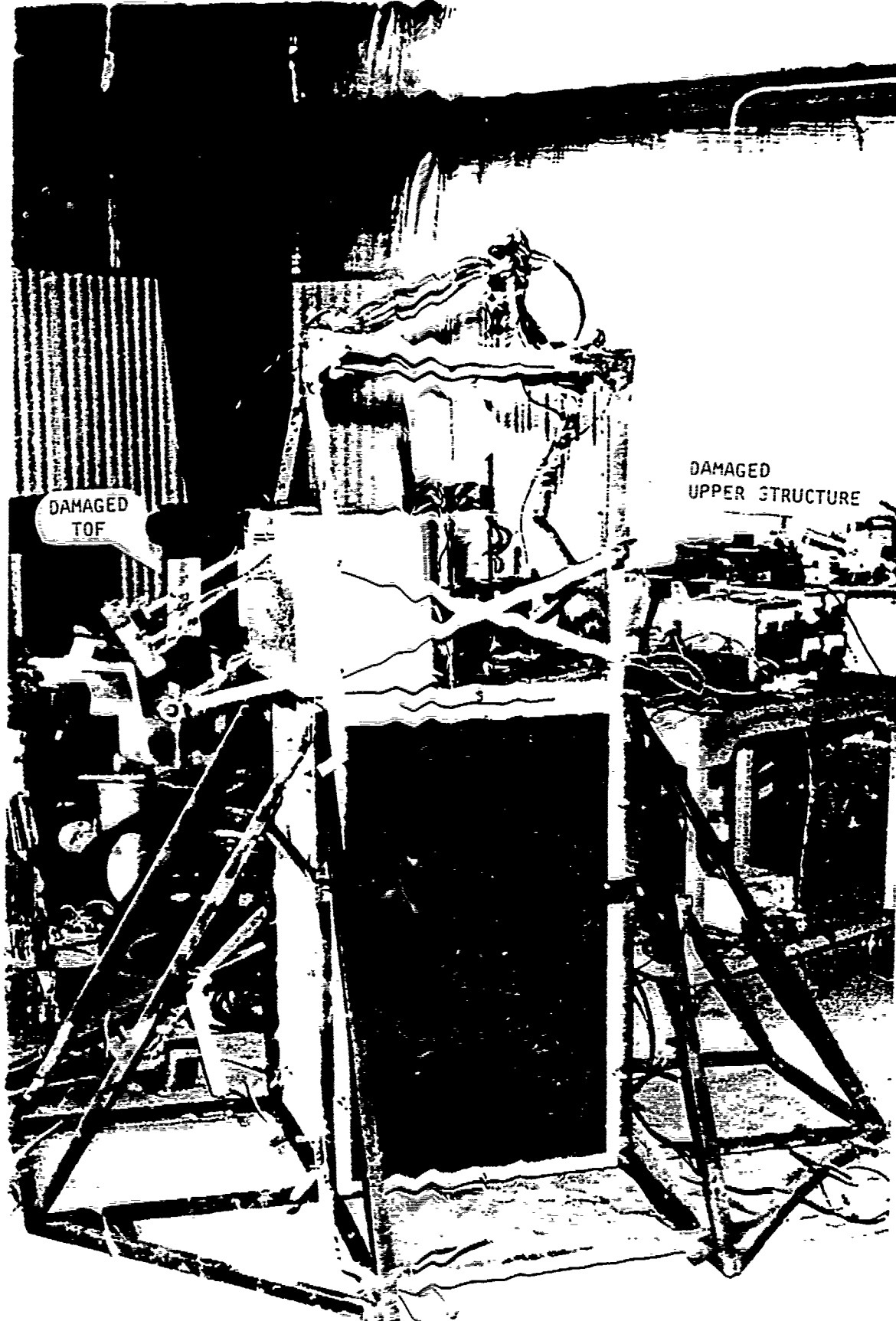


FIGURE 17

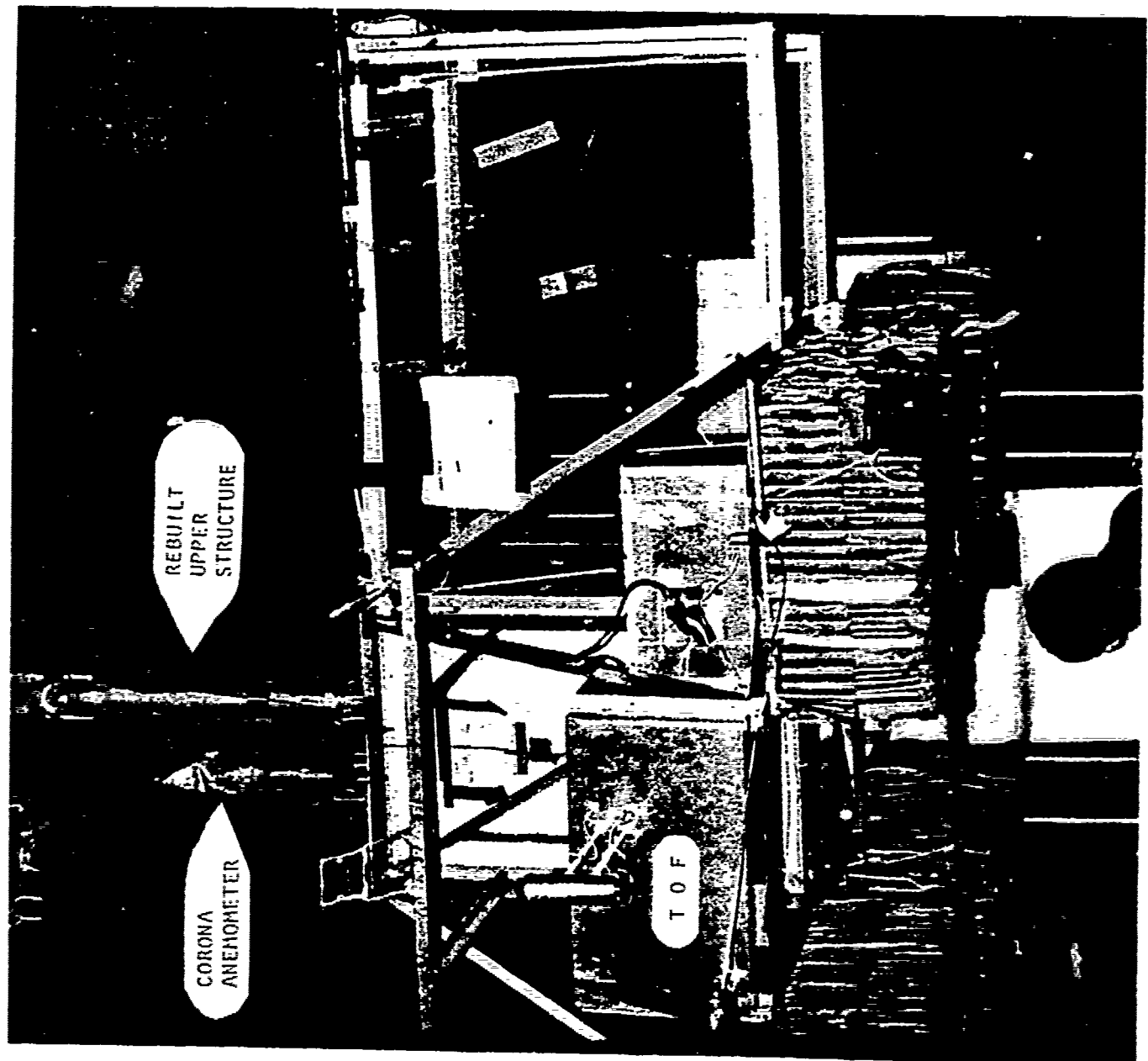
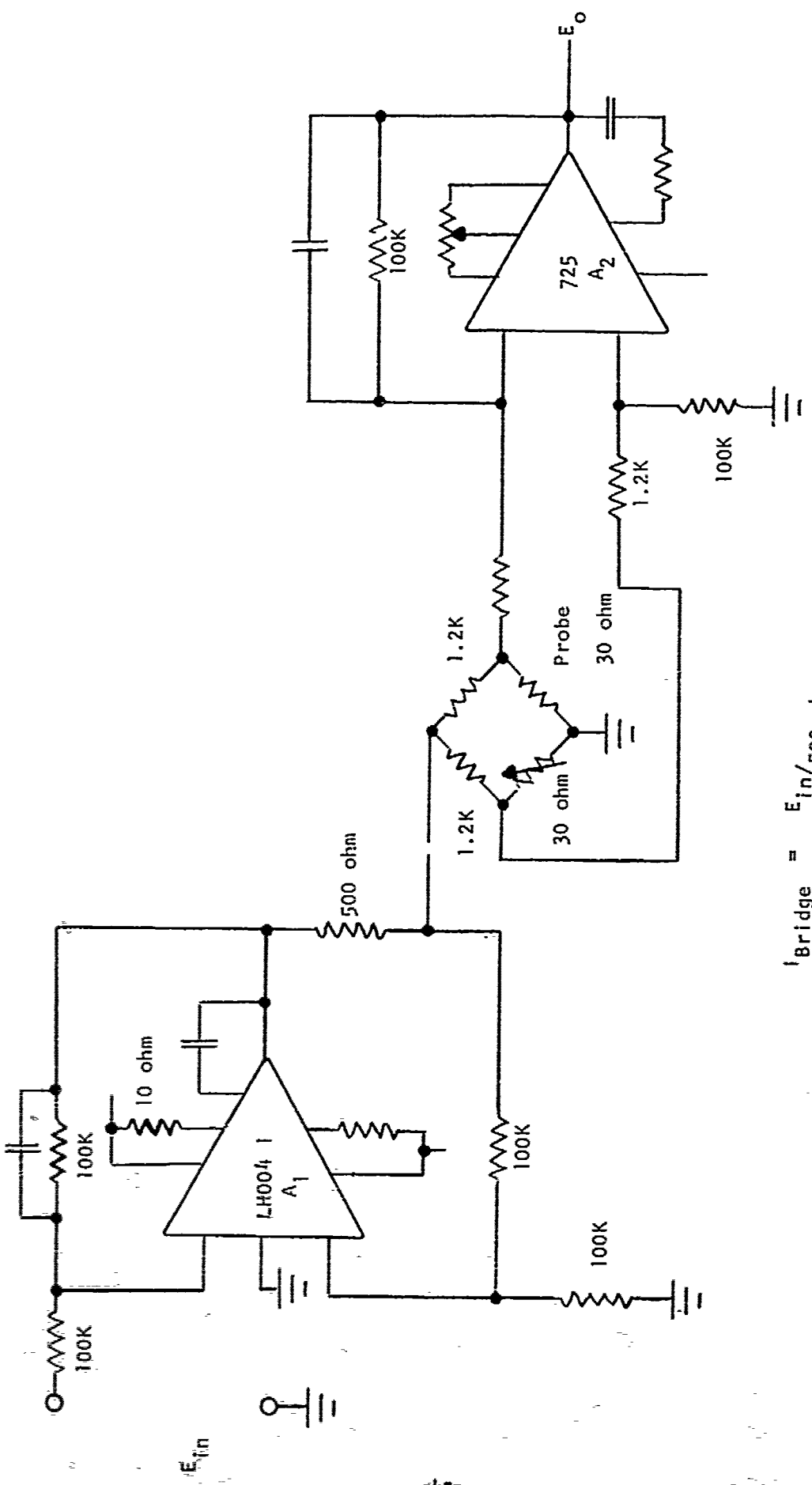


FIGURE 18



$$I_{\text{Bridge}} = E_{\text{in}} / 500 \text{ ohm}$$

CONVECTIVE HEAT TRANSFER  
TEST CIRCUIT  
FIGURE 19

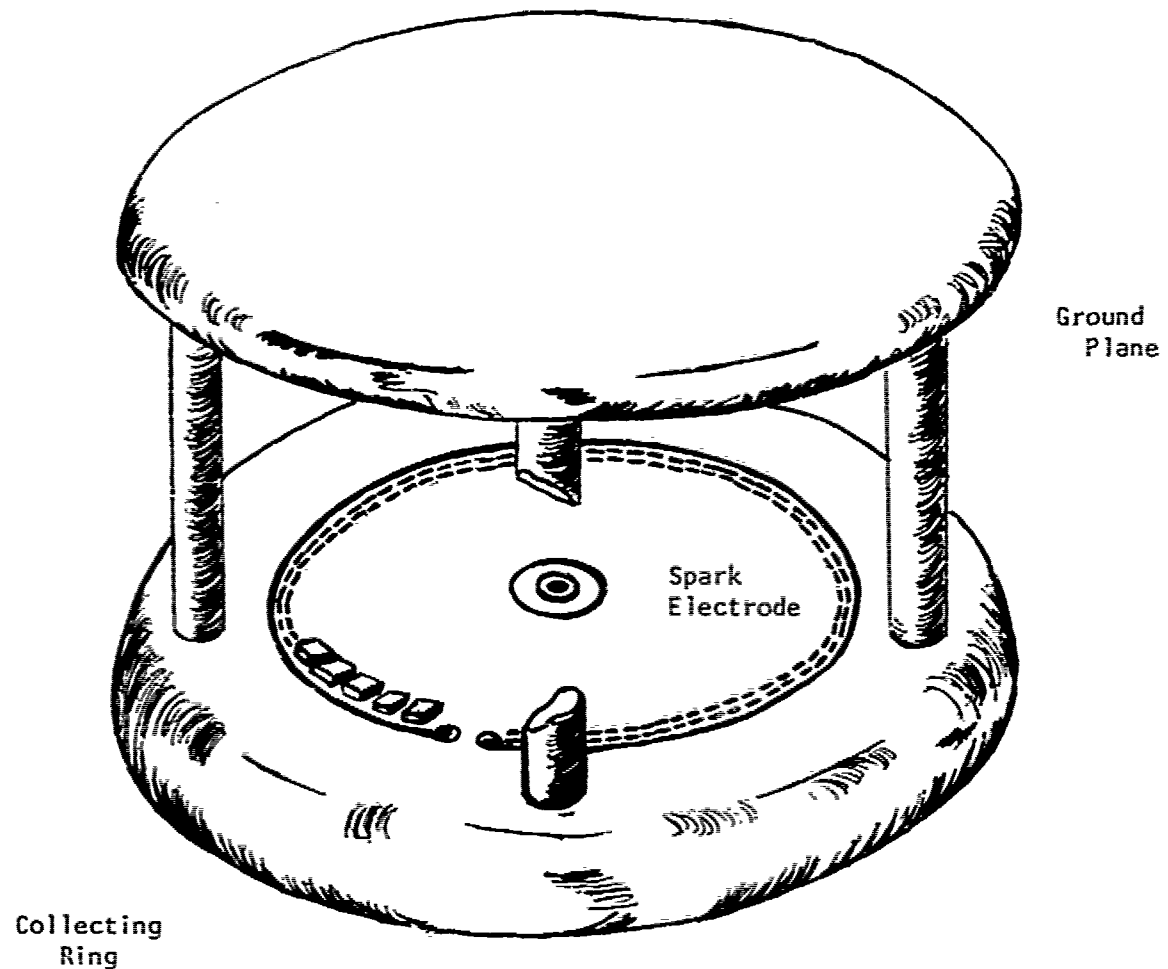
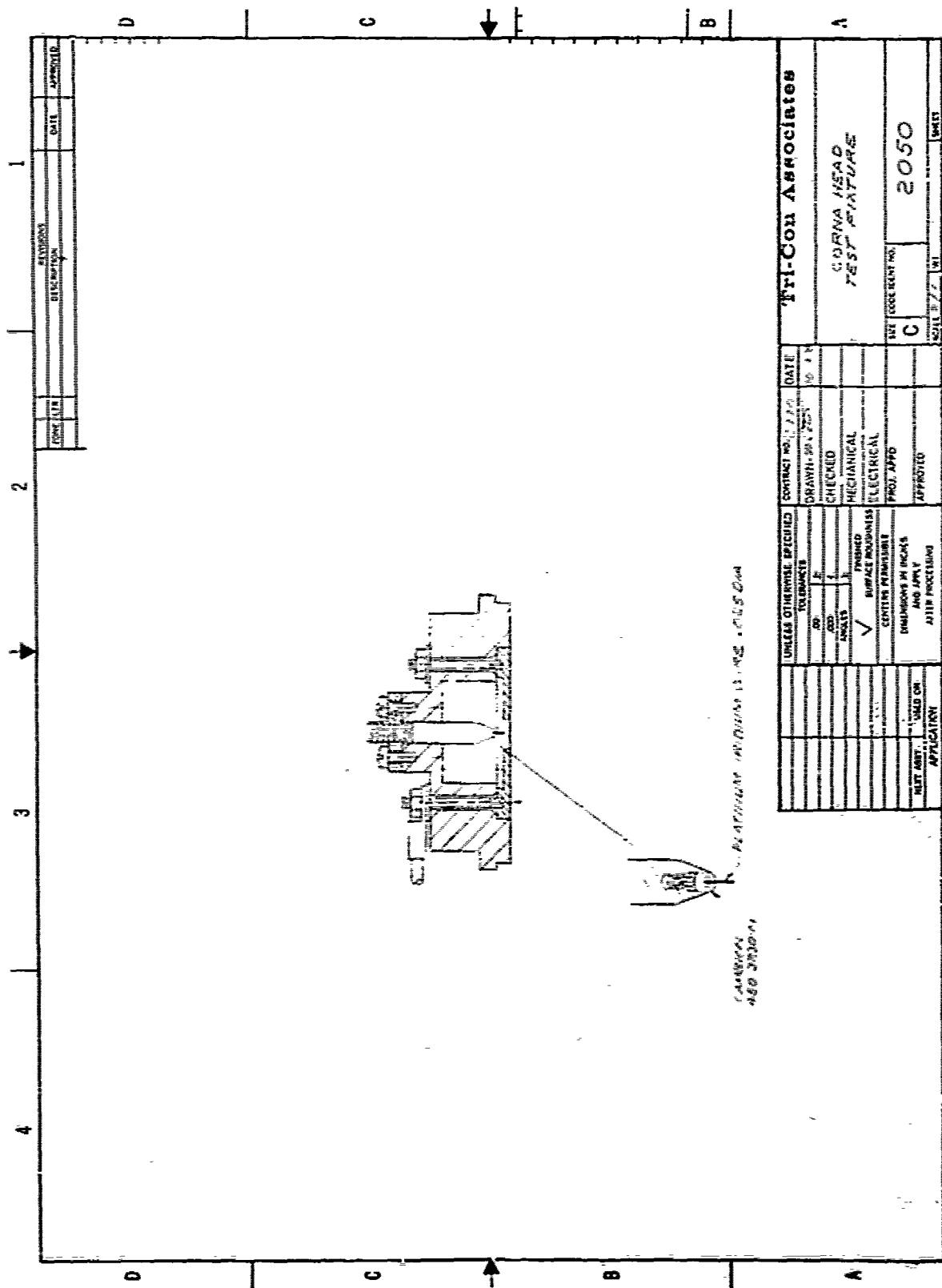
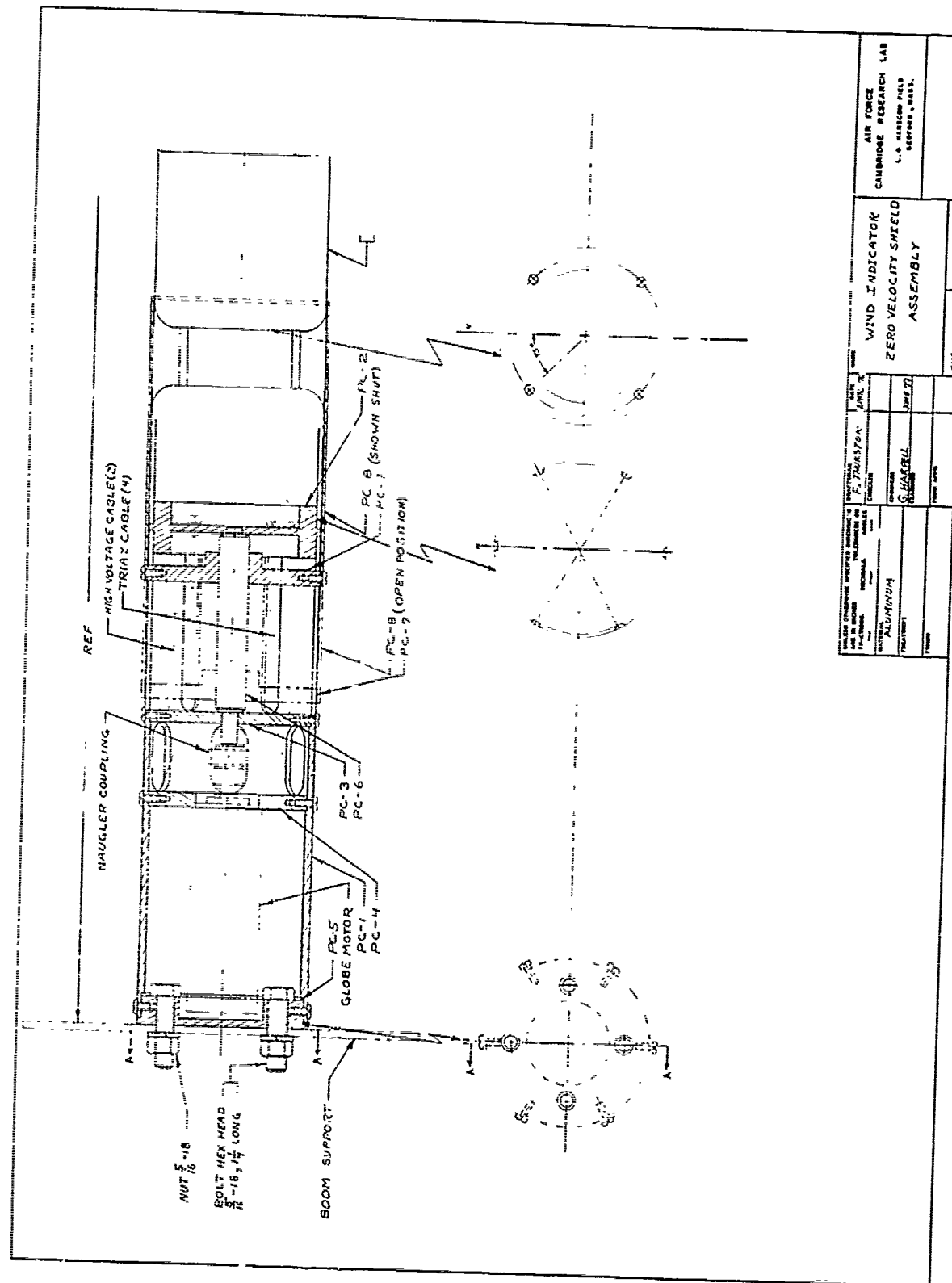
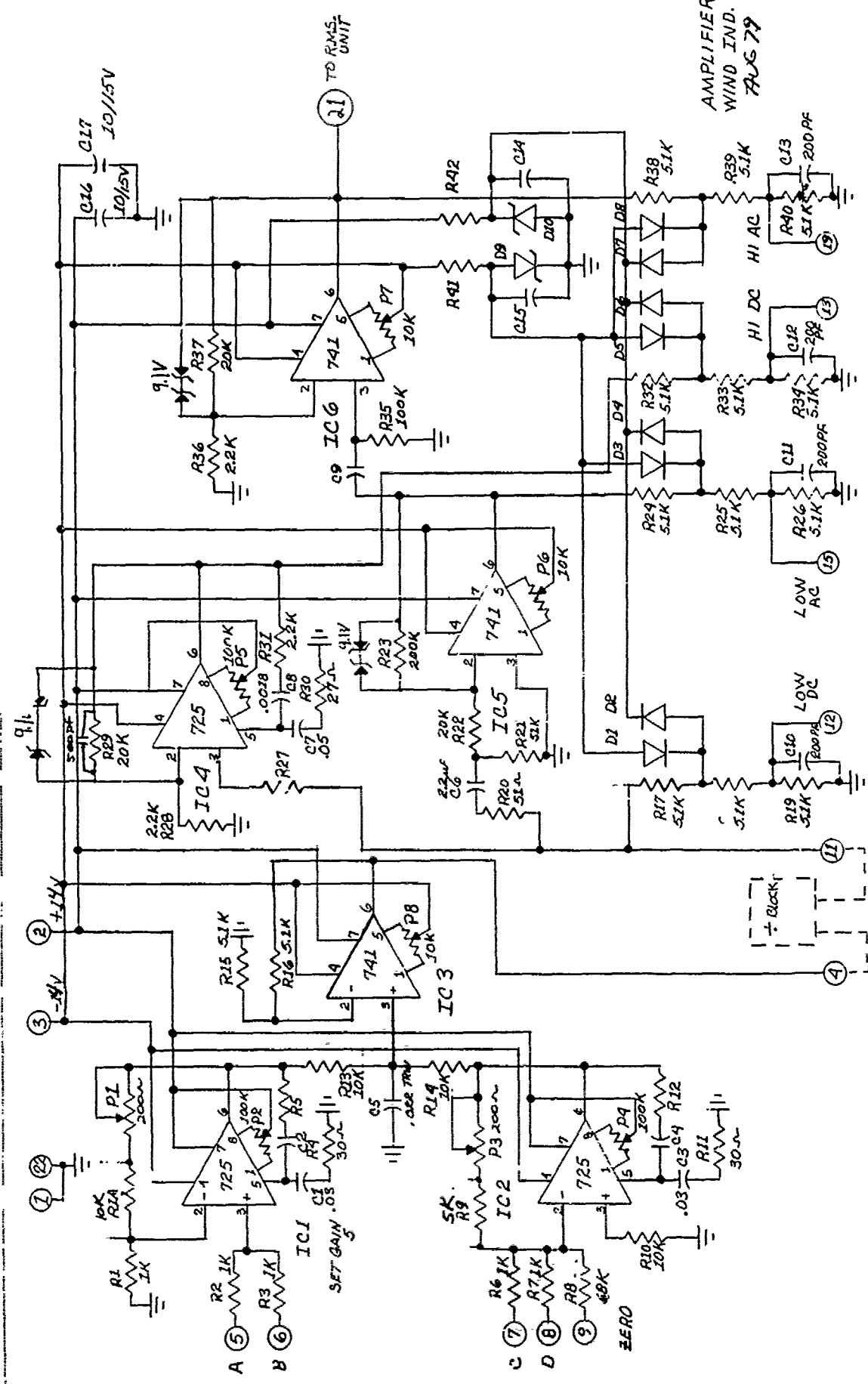


ILLUSTRATION  
Two Dimensional TOF  
FIGURE 20

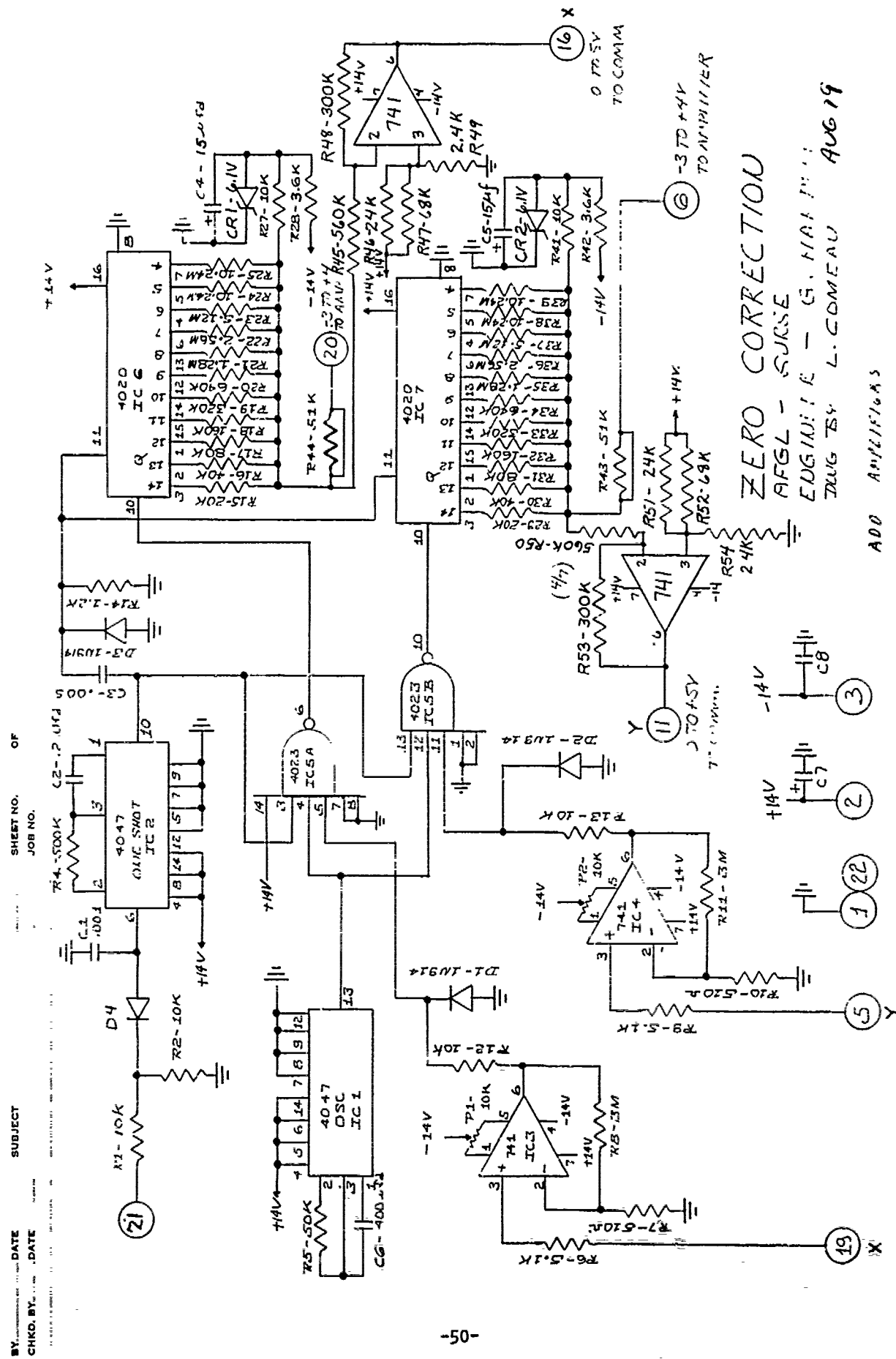




BY	DATE	SUBJECT	SHEET NO.	OF
CKD. BY	DATE	EDR SPILLER PLATE	JOB NO.	1

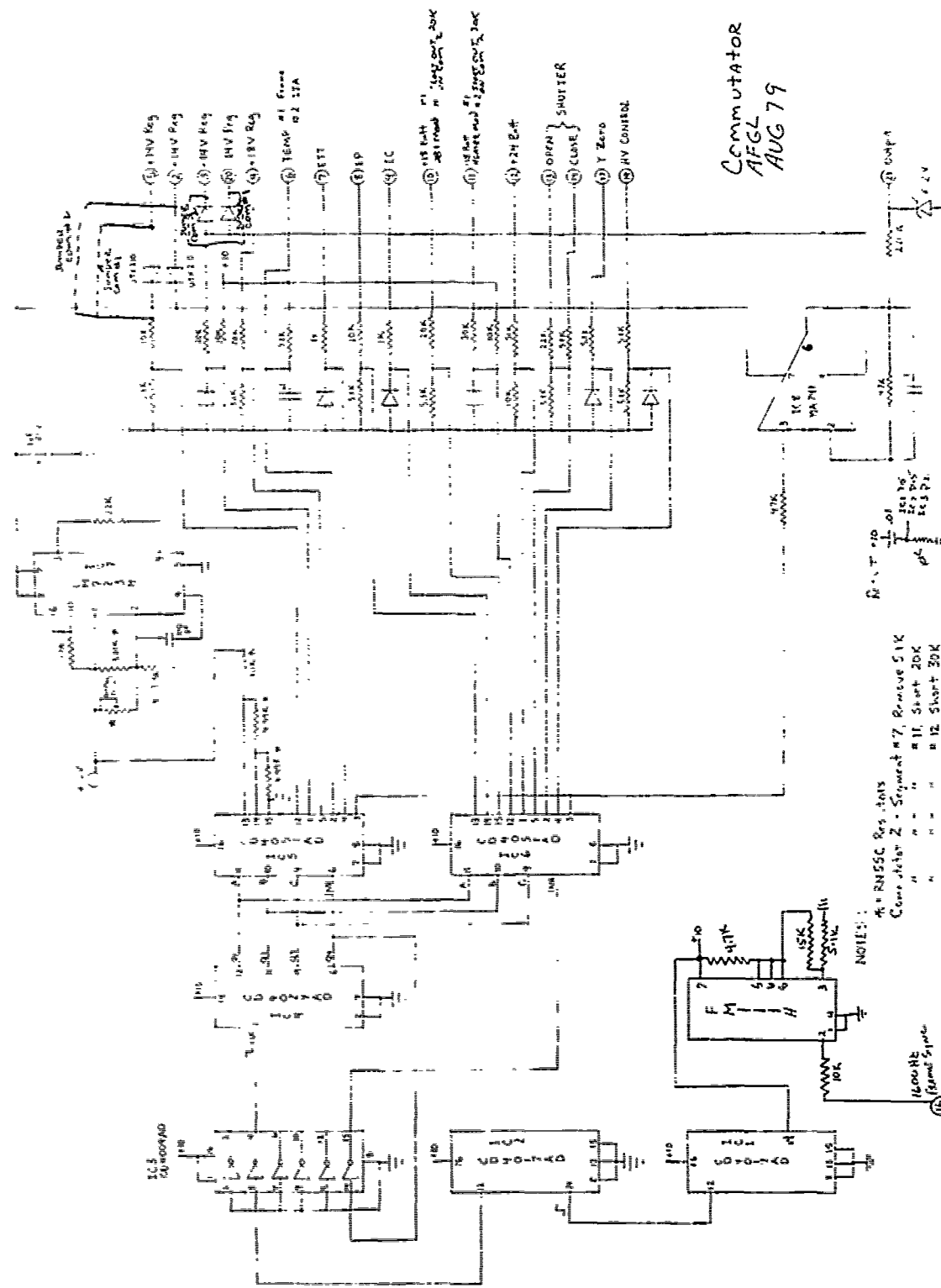


-49-









Commutator  
AEG  
AUG 19

卷之三

Fig. 1.  $R_{\text{eff}} \times 10^{-10}$  vs.  $\tau$  for  $\text{Fe}_{33}\text{P}_{67}$  at  $1000^\circ\text{C}$ .

$$F_0 = \frac{1}{2} \pi^2$$

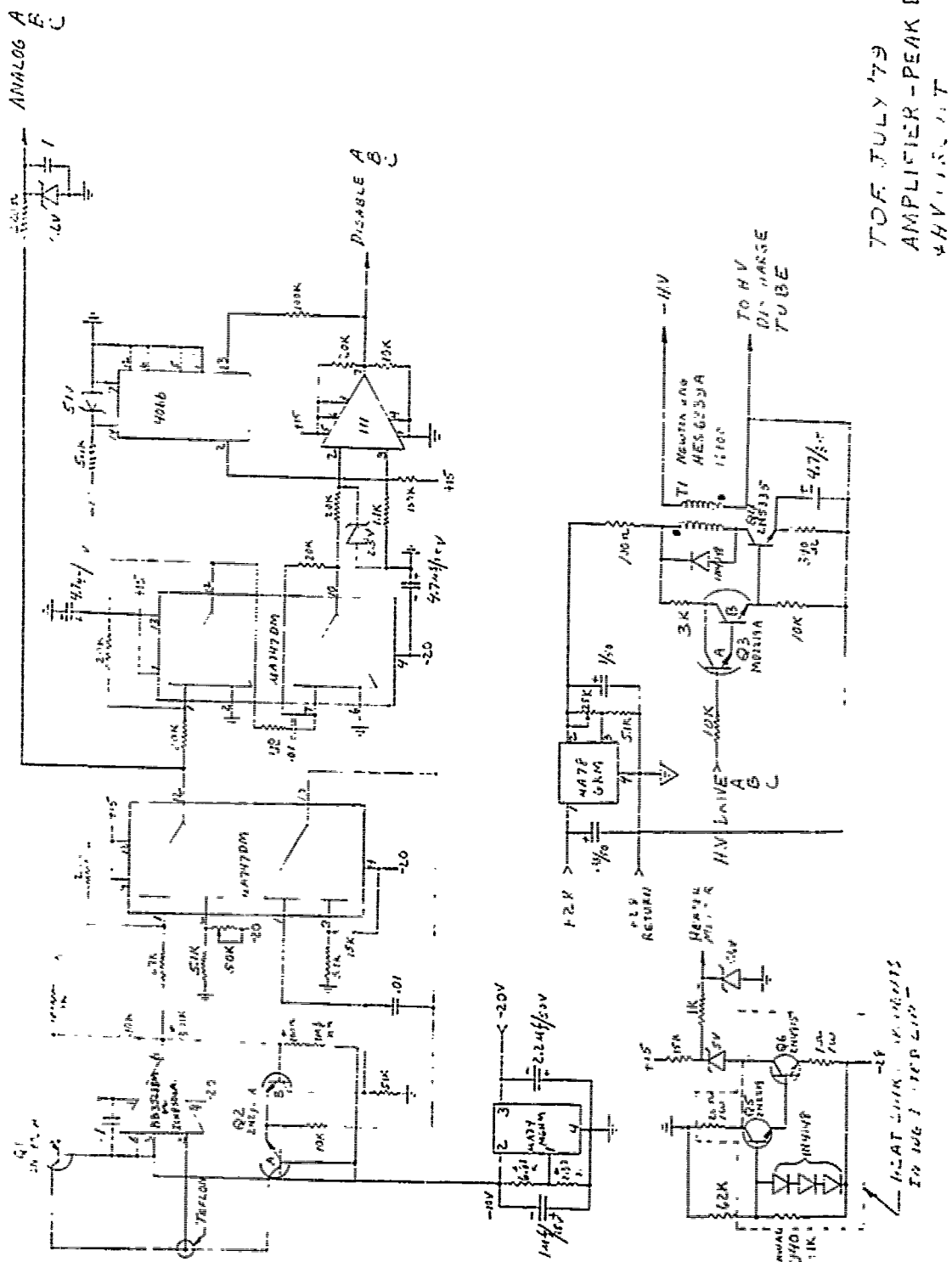
7. Revenue \$ 14

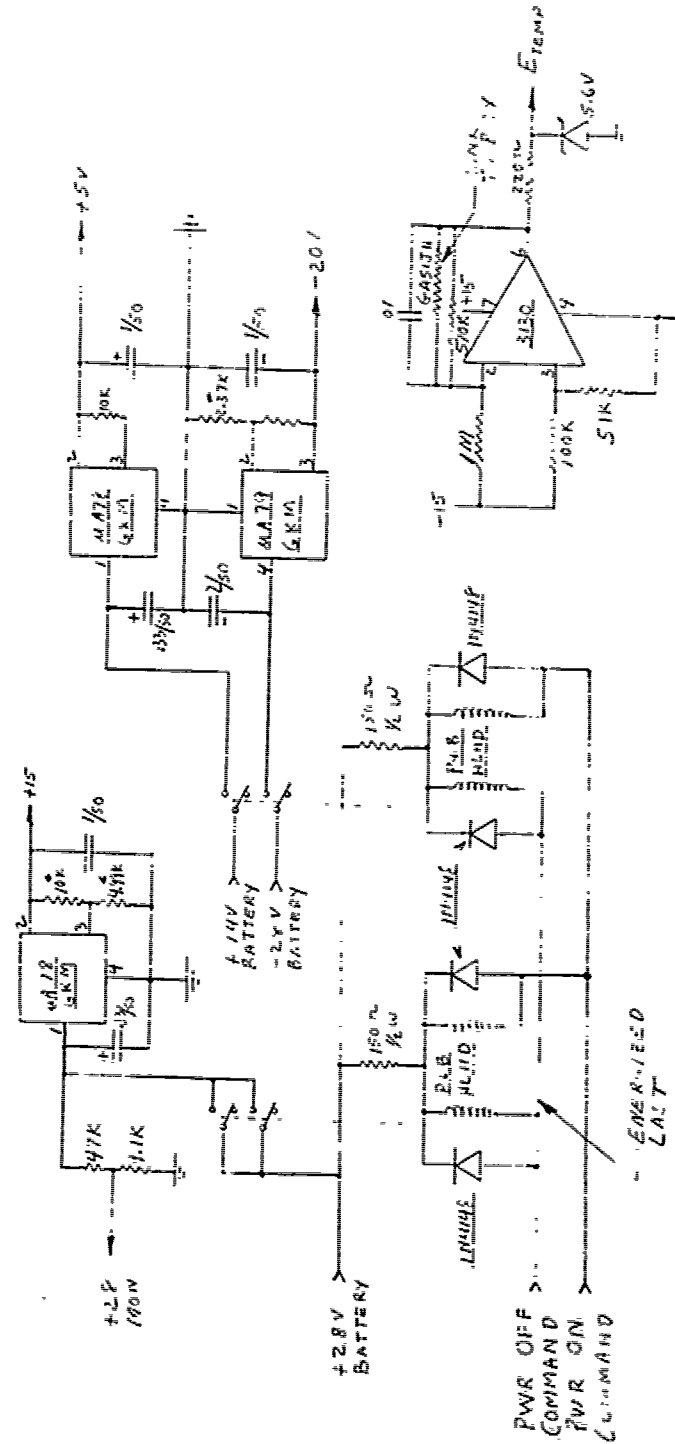
SSC Results -  
Iteration 2 - Segment 1

NO. 11211  
R.M. 1000  
Geneva

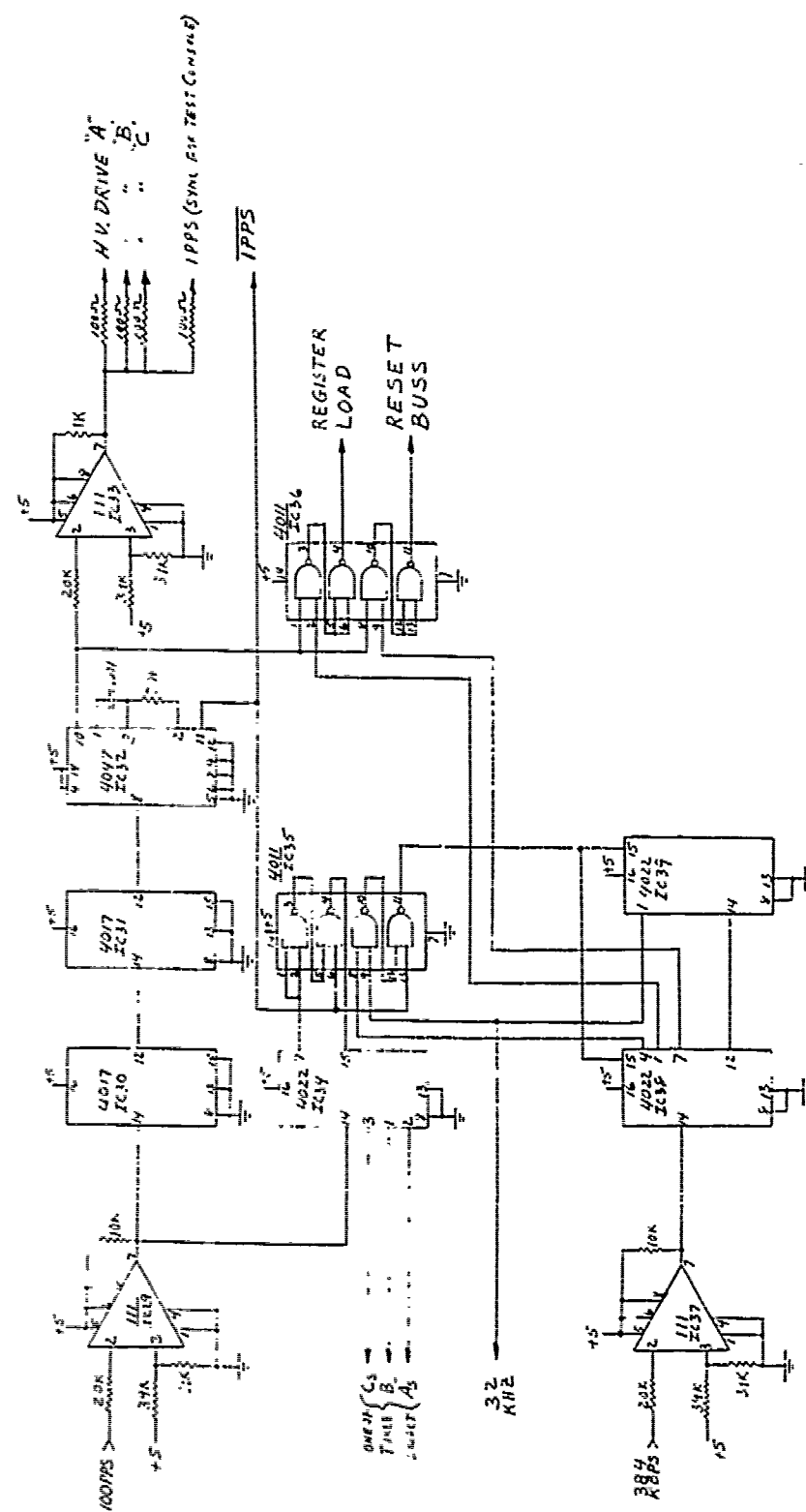
二  
三

111

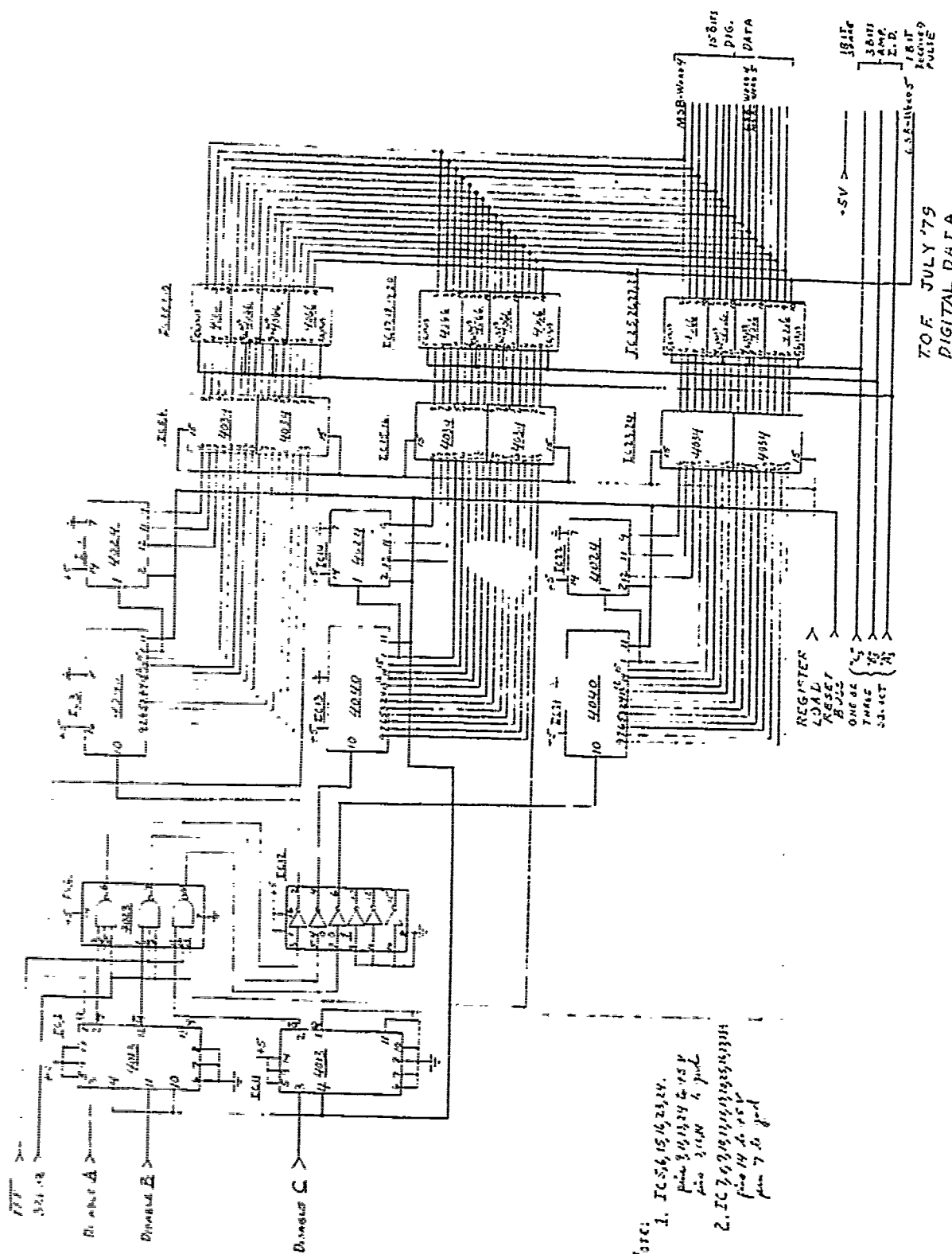


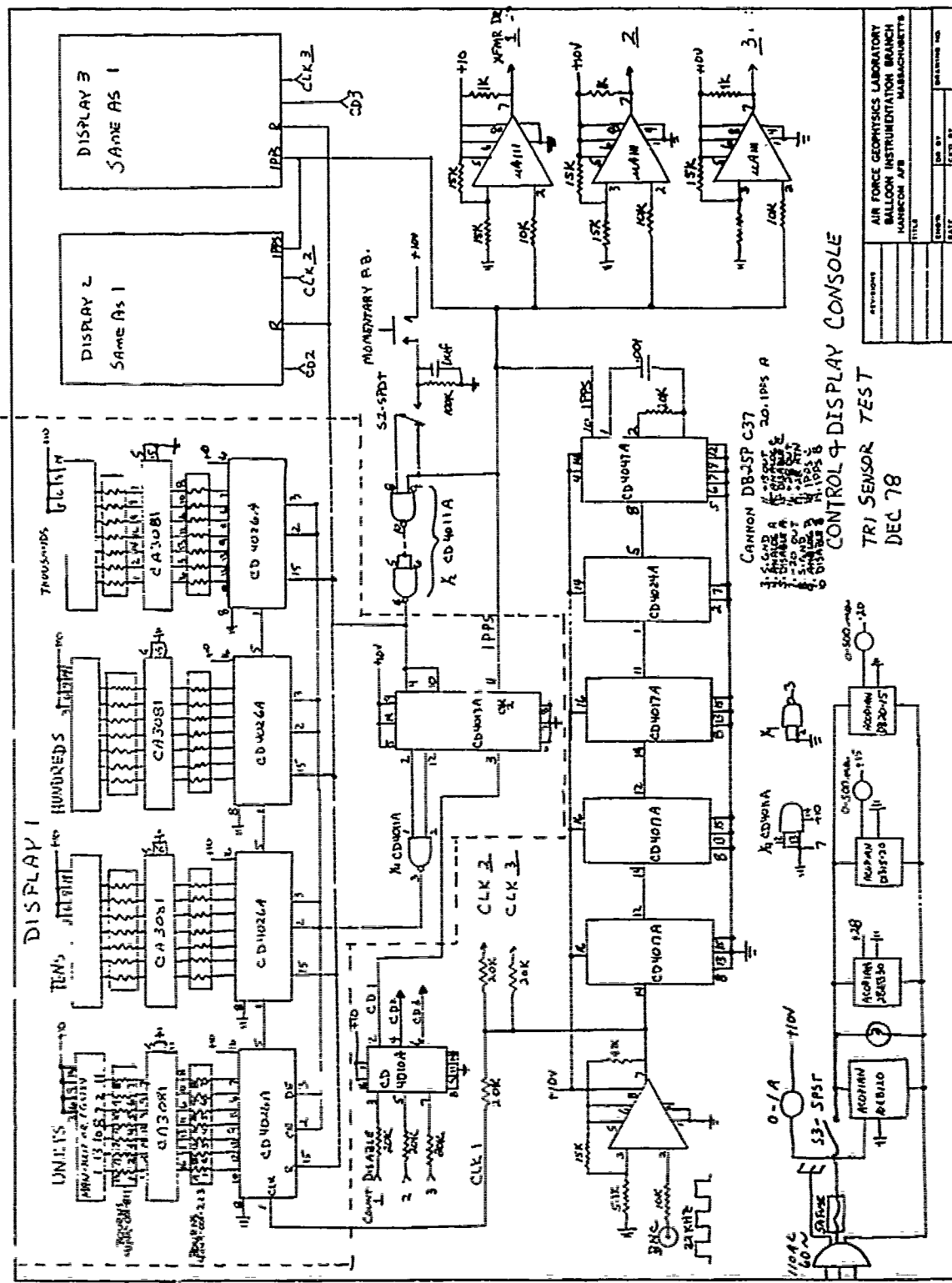


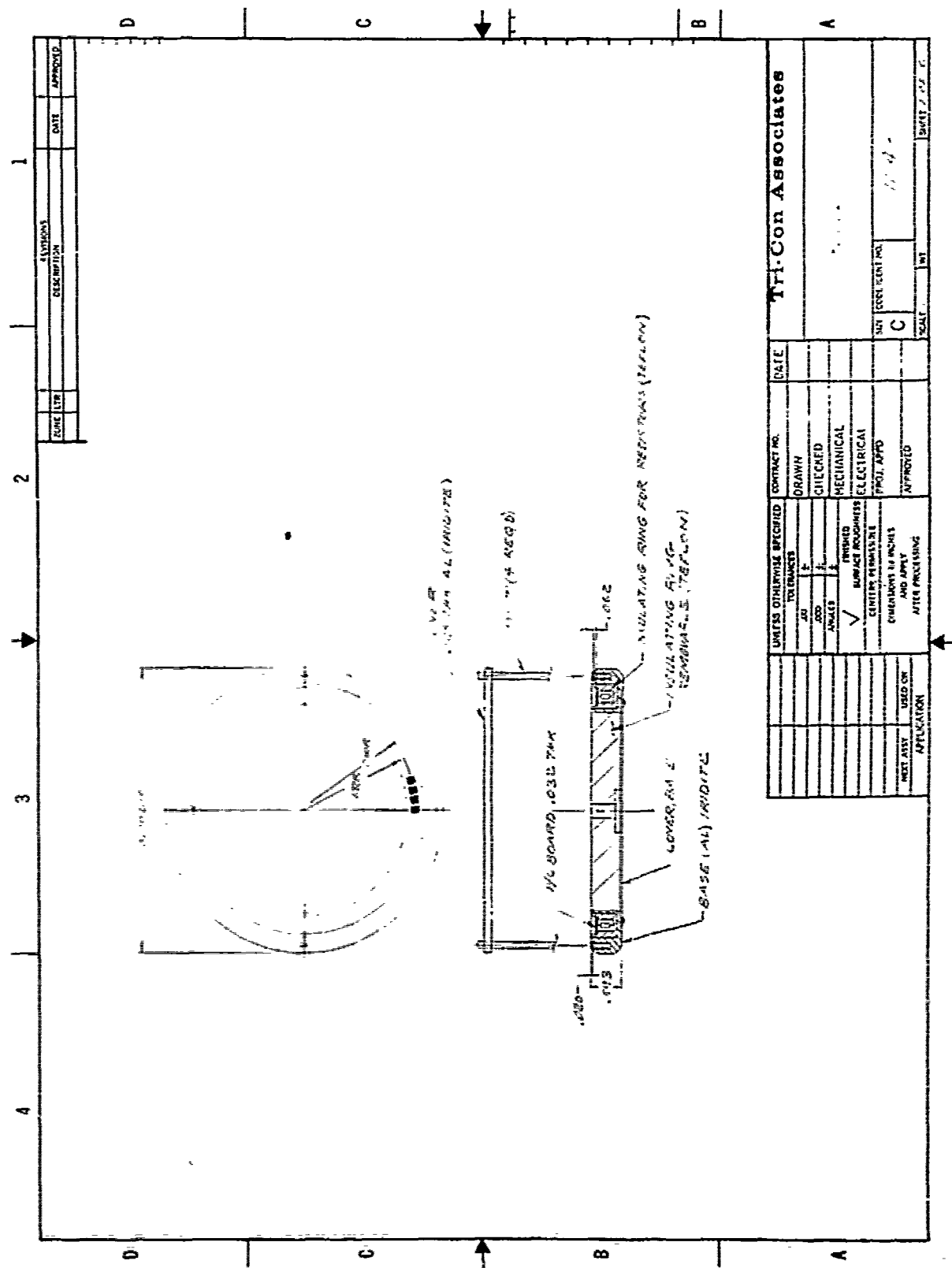
T.O.F. JULY '79  
POWER CONTROL  
+ ETC. (1979)

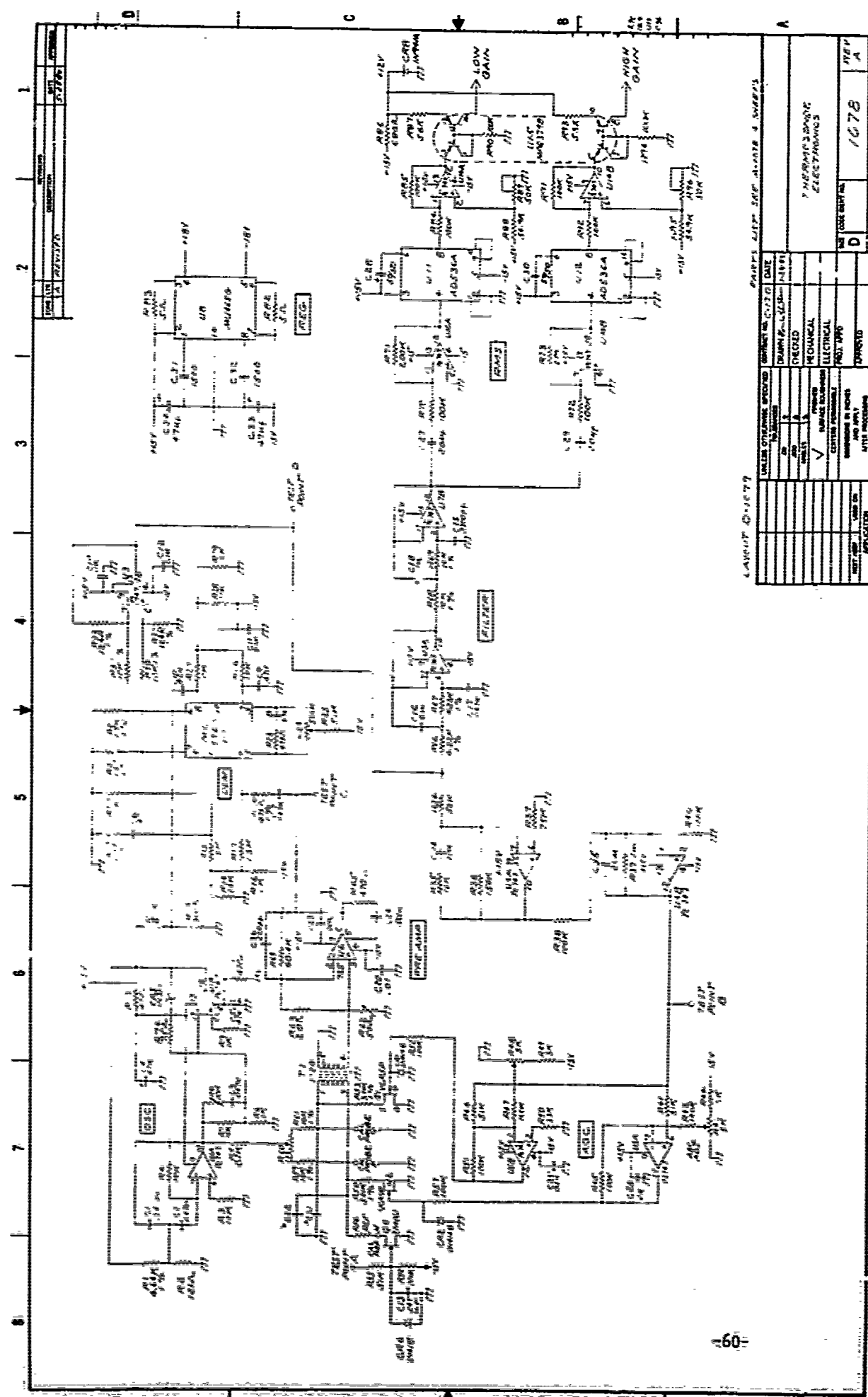


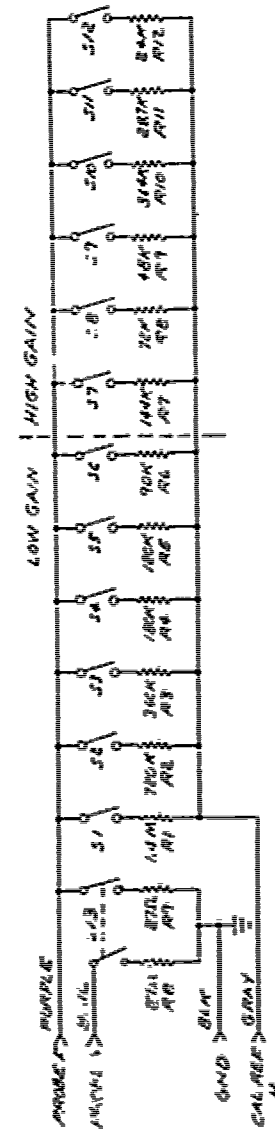
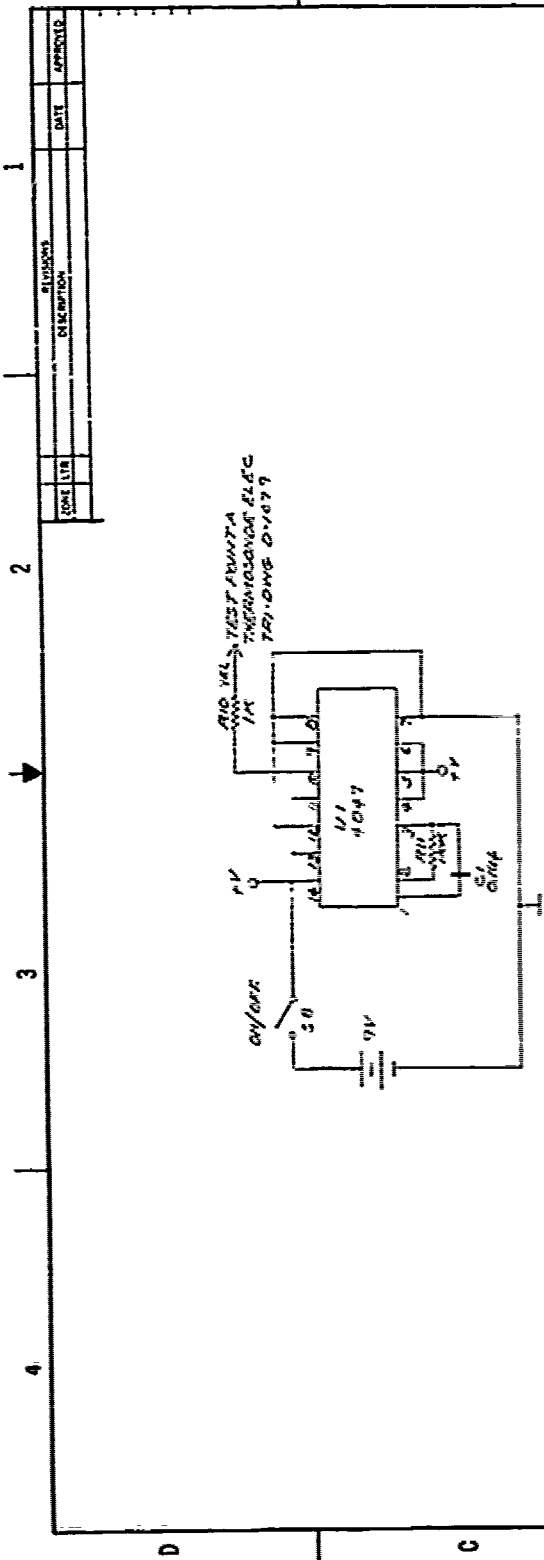
T.O.E. JULY '79



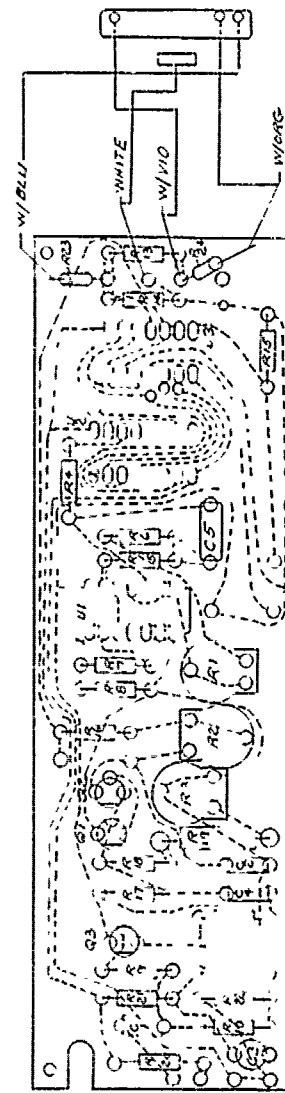


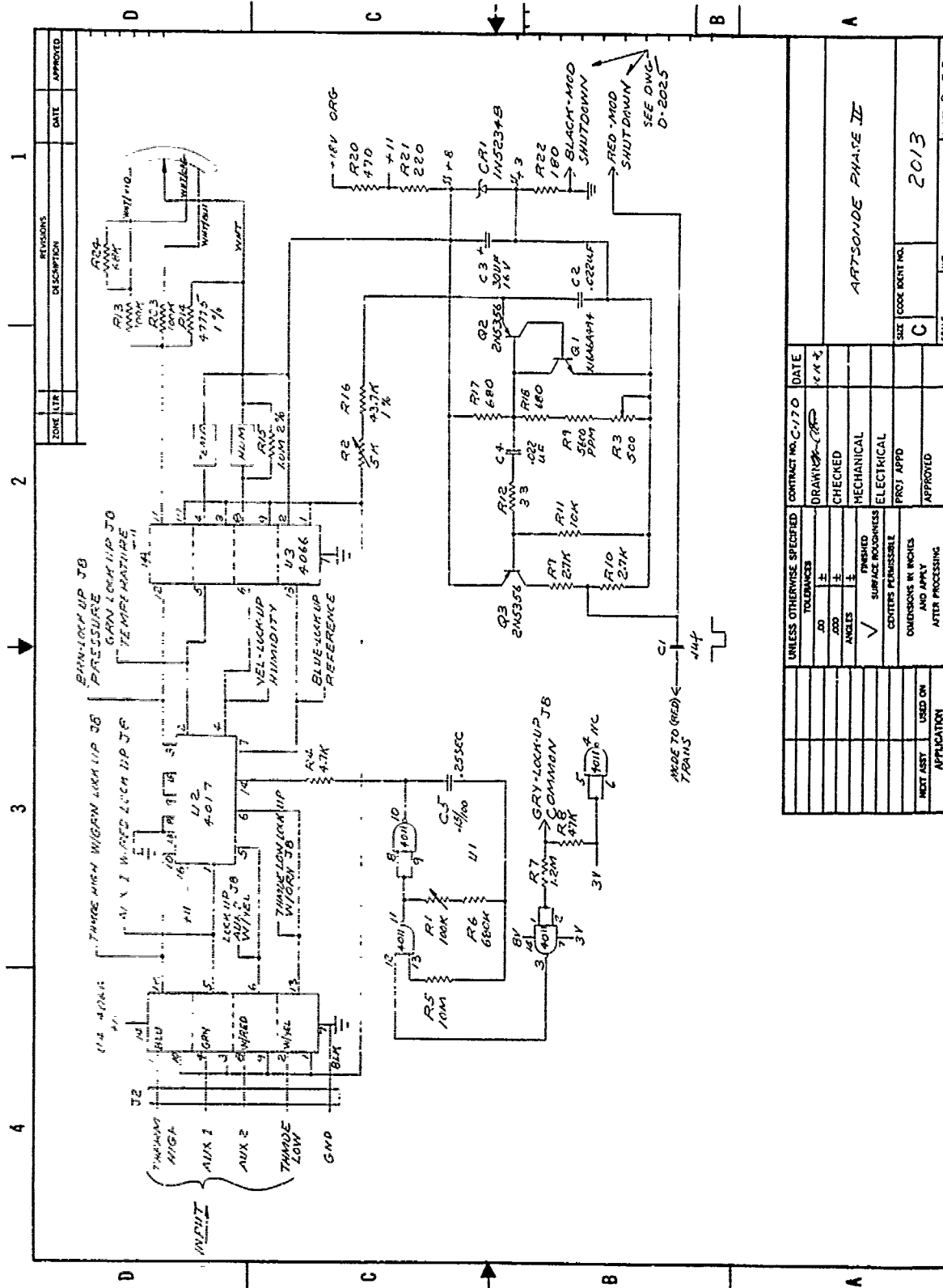


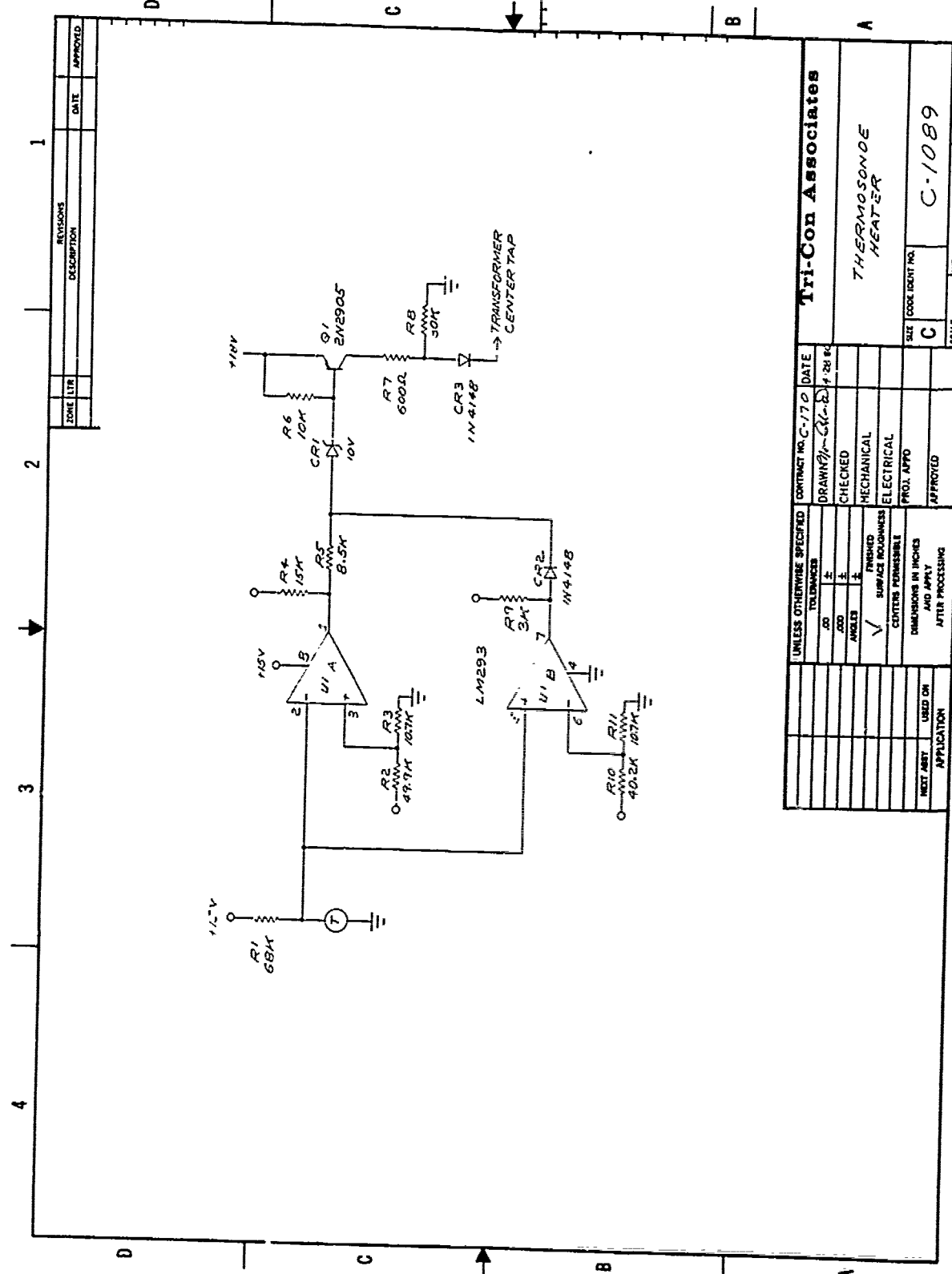


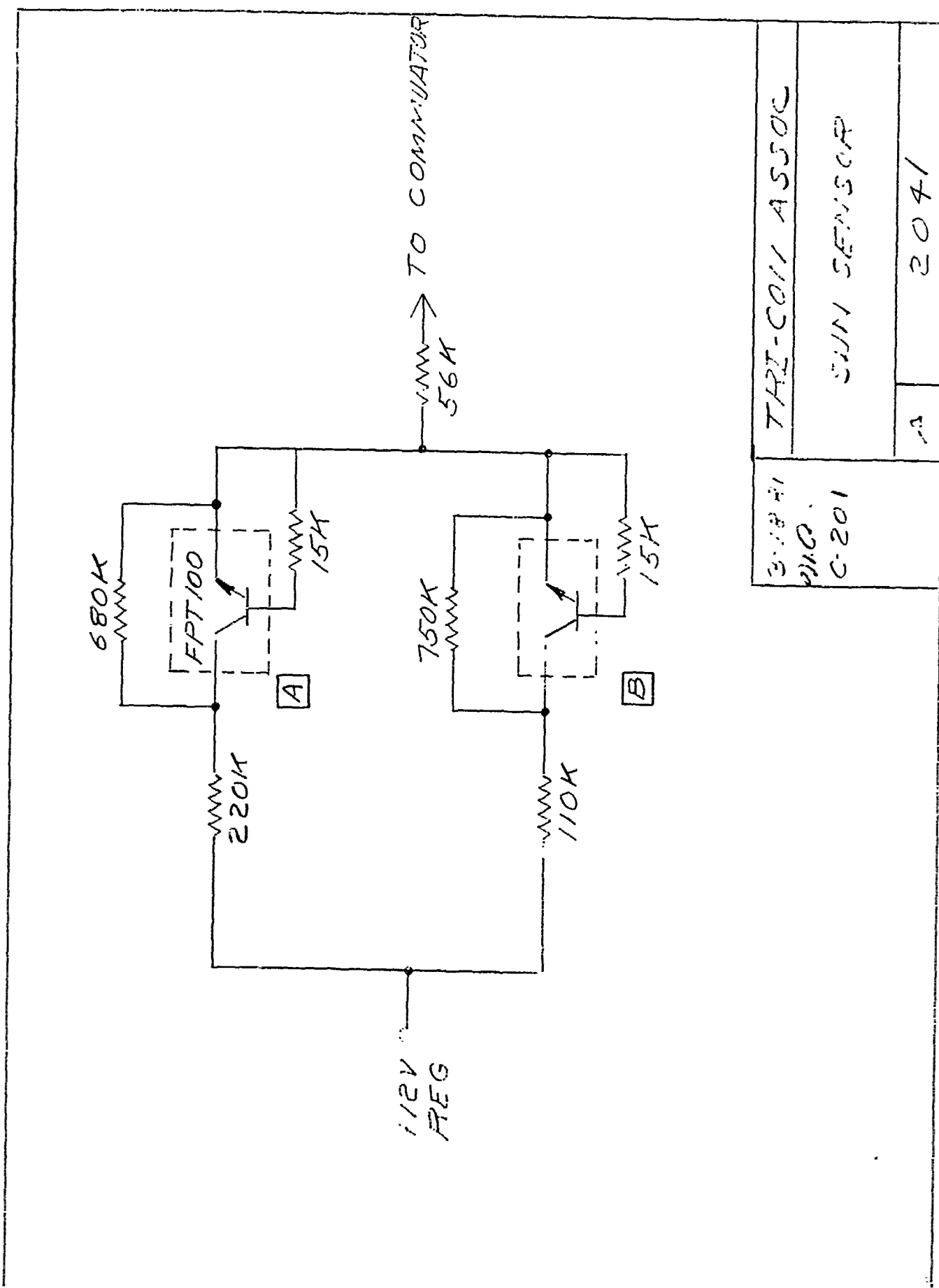


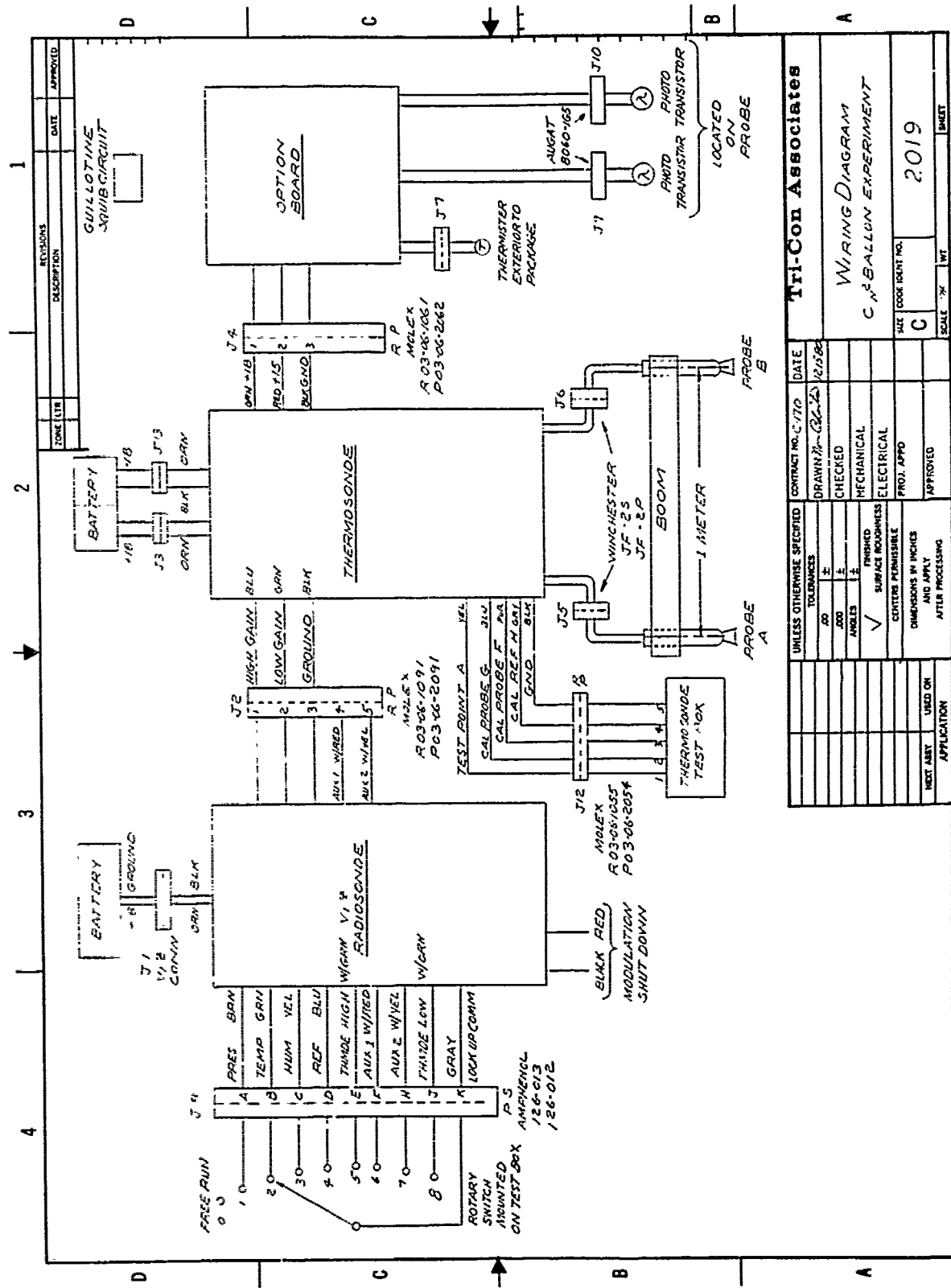
1		2		3		4	
STORY	LIN	REVISIONS	DATE	STORY	LIN	REVISIONS	DATE
		DESCRIPTION	APPLIED				

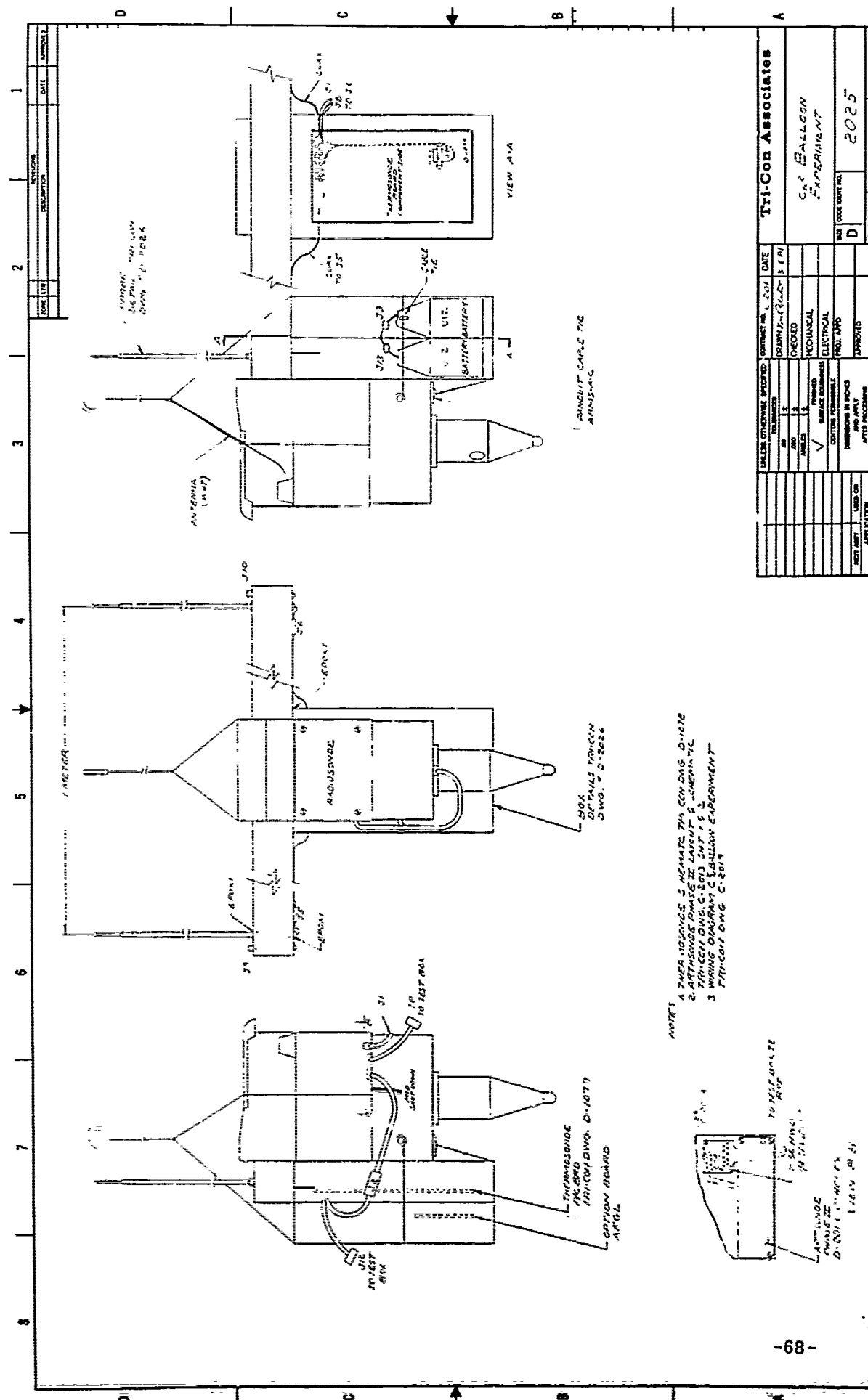












ADDENDUM A

Pre-amp transfer functions from Figure 5:

$$I_{A,B,C,D} = 2 E_{A,B,C,D} \times 10^{-7}$$

$$I_{TT} = 2.1 E_{TTP} \times 10^{-7} \text{ Amps}$$

$E_{TTP}$  = Pre-amp  $E_{TT}$

$$I_{TT} = .41 E_{TTCH} \times 10^{-7} \text{ Amps}$$

$E_{TTCH}$  = Commutator Output  
High Pressure

$$I_{TT} = .94 E_{TTCL} \times 10^{-7}$$

$E_{TTCL}$  = Commutator Output  
Low Pressure